Tetraspanin CD151 and integrin α3β1 contribute to the stabilization of integrin α6β4-containing cell-matrix adhesions

Lisa te Molder[1], Juri Juksar[1,2], Rolf Harkes[1], Wei Wang[1], Maaike Kreft[1], Arnoud Sonnenberg[1*]

[1]Division of Cell Biology I, The Netherlands Cancer Institute, Plesmanlaan 121, Amsterdam 1066 CX, The Netherlands.

[2]Present address Hubrecht Institute, Utrecht, Uppsalalaan 8, Utrecht 3584 CT, The Netherlands.

*Correspondence and request for materials should be addressed to A.S. (email: a.sonnenberg@nki.nl).

Keywords

Hemidesmosome, tetraspanin, CD151, integrin, plectin, keratinocyte adhesion.

Summary Statement

This study elucidates the role of tetraspanin CD151 in the formation and maintenance of cell-matrix adhesions in epidermal keratinocytes.

Abstract

Tetraspanin CD151 has been suggested to regulate cell adhesion through its association with laminin-binding integrins α3β1 and α6β4; however, its precise function in keratinocyte adhesion remains elusive. In this study, we investigated the role of CD151 in the formation and maintenance of laminin-associated adhesions. We show that CD151, through binding to integrin α3β1, plays a critical role in the stabilization of an adhesion structure with a distinct molecular composition of hemidesmosomes with tetraspanin features. These hybrid cell-matrix adhesions, which are formed early during cell adhesion and spreading and at later stages of cell spreading, are present in the central region of the cells. They contain the CD151-α3β1/α6β4 integrin complexes and the cytoskeletal linker protein plectin, but are not anchored to the keratin filaments. In contrast, hemidesmosomes, keratin filament-associated adhesions that contain α6β4, plectin, BP180 and BP230, do not require CD151 for their formation or maintenance. These findings provide new insights into the dynamic and complex regulation of adhesion structures in keratinocytes and the pathogenic mechanisms underlying skin blistering diseases caused by mutations in the gene for CD151.

JCS Advance Online Article. Posted on 5 September 2019

Introduction

The skin is our largest organ and its barrier function protects us from dehydration and pathogenic infections. To exert these functions, the skin needs to maintain its integrity, for which stable adhesion of basal keratinocytes to the underlying extracellular basal lamina is of paramount importance. This adhesion is largely mediated by hemidesmosomes (HDs), multiprotein complexes that are associated with the keratin intermediate filament system within the cell.

The integrin α6β4, a heterodimeric transmembrane protein, is a main component of HDs. In type I HDs, present in the epidermis, α6β4 binds extracellularly to laminin-332 and intracellularly via two associated proteins, plectin and BP230 (BPAG1e), to the keratin cytoskeleton. Besides α6β4, type I HDs contain two other transmembrane proteins: the tetraspanin CD151 and BP180 (also known as BPAG1 or collagen XVII) (Litjens et al., 2006; Sterk et al., 2000; Walko et al., 2015). In more simple epithelia of the intestine or the mammary gland, a rudimentary form of HDs is present. These type II HDs contain α6β4 and plectin, but lack BP180 and BP230 (Fontao et al., 1997; Uematsu et al., 1994).

In humans, the importance of type I HDs for maintaining skin integrity is underscored by genetic evidence that demonstrates that mutations in any of the six genes encoding HD proteins cause the congenital inherited skin blistering disorder Epidermolysis Bullosa (EB) (Has and Fischer, 2018). Patients carrying null mutations in the genes for the integrin α6 or β4 subunits, or the cytolinker protein plectin, suffer from a severe form of EB, which is indicated by the absence of HDs (Ashton et al., 2001; McLean et al., 1996; Nakamura et al., 2005; Niessen et al., 1996; Vidal et al., 1995). However, HDs with grossly normal HD structures, but reduced keratin filament association, are found in patients carrying mutations in the genes for BP180 or BP230, and accordingly, these patients only suffer from a mild form of EB (Groves et al., 2010; Jonkman et al., 1995; Liu et al., 2012; McMillan et al., 1998). Mutations in CD151 have not been associated with abnormalities in HDs but nevertheless cause a mild regional skin blistering phenotype, similar to that observed in patients with mutations in the integrin α3 gene (Crew et al., 2004; Has et al., 2012; Kagan et al., 1988; Vahidnezhad et al., 2017). Targeted deletion of genes encoding HDs and associated proteins in mice largely recapitulates the pathology observed in humans (Andrä et al., 1997; DiPersio et al., 1997; Dowling et al., 1996; Guo et al., 1995; Sachs et al., 2006; van der Neut et al., 1996; Wright et al., 2004).

Integrin α3β1, another laminin-binding integrin expressed by keratinocytes, is a component of focal adhesions (FAs), but can also be found together with α6β4 in tetraspanin enriched microdomains (TEMs) (also named tetraspanin webs). TEMs are formed by lateral associations of tetraspanins with one another and with other proteins. Incorporation of α6β4 and α3β1 in TEMs is facilitated through binding of their α subunits to CD151 (Hemler, 2005). The association of CD151 with laminin-binding

integrins has been reported to affect integrin-dependent adhesion, migration and signaling (Berditchevski, 2001; Stipp, 2010; Termini and Gillette, 2017).

While it has been shown that CD151 is colocalized with α6β4 in type I HDs, the exact function of CD151 in the formation of these adhesions or other cell-matrix adhesions in keratinocytes is not known (Sterk et al., 2002). In this study, we assessed the contribution of CD151 to the formation and maintenance of laminin-associated adhesion complexes in keratinocytes. In agreement with data obtained from CD151 knockout mice and patients with *CD151* mutations, our findings confirm that CD151 is not critical for the formation of type I HDs. However, we show that CD151 is essential for the maintenance of adhesion complexes in which CD151 is present together with α3β1 and the HD proteins α6β4 and plectin, but which are not associated with the keratin cytoskeleton.

Results

CD151 forms multi-protein complexes with both α3β1 and α6β4 in keratinocytes

Previous studies have shown that CD151 forms stable complexes with the laminin-binding integrins α3β1 and α6β4 (Hemler, 2005; Sterk et al., 2002). We confirmed these findings by reciprocal co-immunoprecipitation (co-IP) assays using two different monoclonal antibodies against CD151 (5C11 and 11G5) and antibodies against the integrin α3 and α6 subunits (Fig. 1A). Furthermore, these assays showed that in PA-JEB/β4 keratinocytes the α6 subunit does not form a heterodimer with β1, which is consistent with the fact that α3β1 and α6β4, but not α6β1, are the major laminin-binding integrins in skin (Sonnenberg et al., 1991) (Fig. 1A). Using immunofluorescence (IF) microscopy, we detected CD151 in a pattern of consecutive arches, in which it is partially co-localized with α3β1. Both α3β1 and CD151 are also found at the cell periphery where they do not colocalize and are present in distinctive adhesion structures (Fig. 1B). Furthermore, both α3β1 and CD151 co-localized with the HD proteins α6β4 and plectin (Fig. 1C,D). In summary, these results confirm that in keratinocytes CD151 binds both α3β1 and α6β4, and is present in adhesion structures that contain characteristics of HDs.

CD151 regulates α6β4 distribution.

To determine to what extent CD151 impacts α3β1 and α6β4-containing adhesion complexes, we abrogated CD151 protein expression in PA-JEB/β4 and HaCaT keratinocytes using CRISPR-Cas9 (KO) and subsequently restored the expression of CD151 by retroviral-mediated gene transfer. Analysis by Western blot (WB) and fluorescence-activated cell sorting (FACS) confirmed the absence and restoration of CD151 expression, and showed that the deletion of CD151 did not affect the expression of α3β1 and α6β4 at the plasma membrane (Fig. 2A,B). However, quantitative IF staining and confocal microscopy showed reduced clustering of α3β1 (and to a lesser extent of α6β4) at the basal cell surface

(Fig. 2C). Furthermore, α3β1 was no longer co-distributed with α6β4 but showed increased co-localization with phospho-paxillin in FAs (Fig. 2D,E). In the CD151-proficient cells, α6β4 was clustered in central and peripheral adhesions, but strikingly in the CD151-deficient cells it was almost exclusively present at the cell's periphery (Fig. 2F-H). These results show that, while not essential for α3β1 or α6β4 protein expression or their transport to the plasma membrane, CD151 is necessary for proper organization of these integrins in the central region of the cells.

CD151 is essential for the maintenance of central α6β4-containing-adhesions

To gain real-time insight into how CD151 contributes to the formation of α6β4-containing adhesions in the central region of the cells, we deleted CD151 in PA-JEB keratinocytes expressing GFP-tagged β4 (Geuijen and Sonnenberg, 2002). The absence of CD151 and presence of β4-GFP was confirmed by FACS and WB analysis (Fig. 3A,B). With these cells, the clustering of β4-GFP was followed over time by time-lapse imaging. During initial stages of cell spreading, both CD151-deficient and -proficient PA-JEB/β4-GFP cells assembled α6β4-containing adhesions at the periphery of the keratinocyte islands. However, while these initial adhesion structures were maintained during later phases of cell spreading and island formation in the CD151-proficient cells, in the CD151-deficient cells, the central adhesion structures resolved and disappeared when the cells formed new peripheral adhesions after cell division and cell spreading (Fig. 3C; Movie S1,2). Furthermore, in fluorescence recovery after photobleaching (FRAP) experiments, a spot in the central and peripheral α6β4-containing adhesions was simultaneously bleached and the recovery of the β4-GFP signal at these spots was followed over time (Fig. 3D,E). The results show that the mobile fraction of α6β4 in the central α6β4-adhesions is larger than in the peripheral ones, indicating a higher dynamic nature of α6β4 in the central adhesions (Fig. 3E,F).

Peripheral but not central α6β4-adhesions contain BP230 and are associated with keratin.

We reasoned that the observed differences in the dynamics of α6β4 between central and peripheral adhesion clusters could be due to the association of α6β4 with different proteins. Analysis of the distribution of laminin-332 and plectin by total internal reflection fluorescence (TIRF) microscopy showed that both proteins are associated with central and peripheral α6β4-containing adhesions, with laminin-332 being slightly more abundant under the central adhesion clusters and plectin at the peripheral adhesion clusters (Fig. 4A,B). Strikingly, keratin and BP230 (which, like plectin, can connect α6β4 to the keratin cytoskeleton) were associated solely with α6β4 in the peripheral adhesions (Fig. 4A,B). Interestingly, in the peripheral adhesions only approximately 30 and 50 percent of α6β4 was found to be associated with BP230 and keratin, respectively (Fig. 4B). The possibility that the peripheral adhesions lacking keratin and BP230 are associated with the IF protein vimentin can be largely

excluded since few PA-JEB/β4 keratinocytes express vimentin and even fewer cells have it associated with peripheral adhesions. For similar reasons, we can exclude that the central adhesions are associated with vimentin (Fig. S1). F-actin, which in many PA-JEB/β4 keratinocytes is organized in a typical circumferential ring, was not obviously associated with either the central or peripheral adhesions (Fig. S1). These results characterize many of the peripheral but not the central α6β4-containing adhesions as type I HDs. Consistent with the notion that type I HDs are present in CD151-deficient patients and mice, the HD proteins BP180, BP230 and plectin were all found to co-localize with α6β4 in the peripheral adhesions of CD151-deficient PA-JEB/β4 keratinocytes (Fig. S2). The central α6β4-containing adhesion clusters, which share some of the characteristics of HDs, such as the clustering of α6β4 and its association with laminin-332 and plectin, also have features in common with TEMs: they contain α3β1 and CD151 and therefore display a hybrid molecular composition. From this point forward, we will refer to these adhesions as central HD-like adhesions in this report.

α3β1 is localized in central HD-like adhesions but not in peripheral HDs

Despite the fact that CD151 can form stable complex with both α3β1 and α6β4, type I HDs in the skin contain only complexes of CD151 with α6β4 (Sterk et al., 2002; Underwood et al., 2009). To investigate the distribution of α3β1 in relation to CD151 in the different cell-matrix adhesions in the cultured keratinocytes, we performed TIRF imaging and created intensity profiles along a line segment. As shown in Fig. 4, the intensity plots of CD151 and α6β4 in the central HD-like adhesions and the peripheral HDs almost completely overlapped each other (Fig. 4C). In contrast, the profiles of α3β1 and α6β4 only overlapped in the central HD-like adhesions (Fig. 4C). In the peripheral region the peak intensities of α3β1 overlapped with that of tyrosine phosphorylated FA-associated protein paxillin, and not with HD markers BP230 and keratin (Fig. 4D). These results confirm that central and peripheral adhesions differ in protein composition. Furthermore, while in the central HD-like adhesions α3β1, α6β4 and CD151 cluster together, in the periphery they can be found in two distinct complexes: α3β1 in FAs and α6β4 and CD151 in type I HDs.

CD151 stabilizes central HD-like adhesions through binding to α3β1 and self-association.

Our findings so far indicate that CD151 is essential for maintaining central HD-like adhesions. To determine whether CD151 stabilizes these adhesions through binding to α3β1, we deleted and reconstituted integrin α3 in the HaCaT and PA-JEB/β4 keratinocyte cell lines (Fig. 5A,B; Fig. S3A,B). In both these cell lines, the absence of α3 did not affect the total levels of β4 at the cell surface and the formation of peripheral HDs was not obviously disturbed. However, as observed in the CD151-deficient cells, the absence of α3 caused a loss of central HD-like adhesions, albeit less dramatically (Fig. 5B-D; Fig. S3C). To exclude the possibility that the absence of the central HD-like adhesions is caused by

reduced spreading of the α3-deficient cells, we also analyzed the cells that were plated on coverslips coated with a mixture of vitronectin and fibronectin. Under these conditions, cell spreading of the α3-deficient cells was increased and found to be comparable to that of the wild-type cells on uncoated coverslips. Importantly, the difference in the amount of central HD-like adhesions persisted between the α3-deficient and -proficient cells (Fig. S3D,E).

Next, we investigated whether the role of α3β1 in maintaining the central HD-like adhesions requires binding of α3β1 to laminin-332. To this end, we introduced an α3-binding-deficient mutant (G163A) into the α3-deficient HaCaT cells (Zhang et al., 1999). Expression of the mutant α3β1 was verified by FACS analysis (Fig. 5B). Unlike the wild-type α3 subunit, the α3-G163A mutant was unable to completely rescue the central HD-like adhesions, suggesting that α3β1 binding to laminin contributes to efficient maintenance of these adhesions (Fig. 5C,D). These findings were confirmed in PA-JEB/β4 cells using the α3 blocking antibody, J143 (Fig. S3F,G).

Palmitoylation of CD151 is necessary for stabilization of the CD151 TEMs and hence for incorporation and clustering of α3β1 and α6β4 into these multi-molecular complexes of CD151 (Berditchevski et al., 2002; Yang et al., 2002). To study the role of this self-associating function of CD151 for the stabilization of the central HD-like adhesions, we introduced a CD151 palmitoylation mutant into the CD151-deficient cells (Fig. 5B) (Berditchevski et al., 2002). The expression of this mutant in CD151 KO cells did not rescue the central HD-like adhesions, suggesting that for the maintenance of these clusters CD151 needs to form multi-molecular complexes by oligomerization (Fig. 5E,F; Fig. S3H). Together these results show that for efficient maintenance of the central HD-like adhesions, both laminin-332-associated α3β1 and self-associated and TEM-forming CD151 are needed.

Laminin-332, but not plectin contributes to clustering of α6β4 in central HD-like adhesions.

Since the peripheral HDs and central HD-like adhesions contain more plectin and laminin, respectively, we studied whether CD151-mediated clustering of α6β4 in the different adhesions requires binding of α6β4 to laminin-332 or plectin. Therefore, we expressed the β4 mutants, β4-AD and β4-RW, in the β4-deficient PA-JEB keratinocytes (Fig. 6A). The β4-AD mutant is an adhesion-defective mutant that cannot bind to laminin-332, while the β4-RW mutant, carrying a single missense mutation R1281W in the cytoplasmic domain of β4, is unable to bind plectin (Geerts et al., 1999; Nievers et al., 2000; Russell et al., 2003). In the β4-AD mutant expressing cells, central HD-like adhesions were less commonly present than in the β4-WT expressing cells (Fig. 6B,C). Similar findings were obtained when PA-JEB/β4 and HaCaT cells were treated with the β4 blocking antibody ASC8 (Russell et al., 2003). In the presence of this blocking antibody, the central HD-like adhesions are mostly absent, while there are abundant peripheral HDs (Fig. 6D,E). In the cells expressing the β4-RW mutant and in plectin-deficient PA-JEB/β4 keratinocytes, the α6β4 staining was diffused and adhesions were less well-defined. Nevertheless, in

many cell islands some central HD-like adhesions could be observed (Fig. 6B,C,F,H). In addition, the loss of plectin resulted in a reduction of peripheral HDs (Fig. 6G,H). These results, indicate that the binding of α6β4 to laminin-332, like that of α3β1, contributes to the stabilization of the central HD-like adhesions. On the contrary, binding of α6β4 to plectin is not essential, but might contribute to the clustering of this integrin in the peripheral type I HDs.

CD151 does not affect the strength of α6β4-mediated cell adhesion

Integrin clustering determines the strength by which cells adhere to the ECM (Puklin-Faucher and Sheetz, 2009). To investigate whether CD151-mediated clustering of α3β1 and α6β4 strengthens the adhesion of keratinocytes to laminin-332 deposited by the cells to the substratum, we quantified the adhesion strength of CD151-proficient and -deficient HaCaT keratinocytes, which express both α3β1 and α6β4, using a spinning disk device (Boettiger, 2007). CD151-deficient cells showed a reduced tolerance (albeit not statistically significant) to shear stress compared to the proficient cells (Fig. 7A), suggesting that CD151 plays only a minor role in adhesion strengthening when both α3β1 and α6β4 are present. Next, we investigated whether cell adhesion mediated by either α3β1 or α6β4 is strengthened by CD151. To resolve this, we individually deleted α3 and β4 in the CD151-deficient HaCaT keratinocytes and confirmed the absence of these proteins by FACS and WB analysis (Fig. 7B,C). The deletion of α3 in the CD151-deficient HaCaT keratinocytes had no effect on the adhesive strength of α6β4 to laminin-332 (Fig. 7D). However, in the absence of α6β4, the additional loss of CD151 resulted in a significant reduction in α3β1-mediated adhesion strengthening (Fig. 7E,F). We conclude that CD151 significantly strengthens α3β1, but not α6β4-mediated cell adhesion by facilitating the clustering of this integrin into central HD-like adhesions.

Discussion

CD151 has been shown to be broadly expressed by a variety of cell types and to form complexes with different laminin-binding integrins, including α3β1 and α6β4 (Sincock et al., 1997). In skin, CD151 is complexed with α6β4 and is a component of HDs (Sterk et al., 2000). In this study, we show that in cultured keratinocytes CD151 is not only present in HDs, but also in an adhesion structure with a distinct molecular composition of a HD with tetraspanin features. These hybrid adhesion structures, which are present in the central region of the cell, and referred to as central HD-like adhesions, contain in addition to the CD151-α3β1/α6β4 integrin complexes the cytolinker plectin, but are not associated with keratin filaments. We further show that CD151, through its binding to α3β1 is critical for the formation and stabilization of these central HD-like adhesions and strengthens α3β1- but not α6β4-

mediated keratinocyte adhesion to laminin-332. CD151 is not needed for the formation of type I HDs that are formed in the periphery of the cells and are anchored to keratin filaments (Fig. 8).

The mechanistic reasons for the lack of association of keratin filaments with the central HD-like adhesions, can be surmised based on previous studies. PKA-mediated phosphorylation of plectin at S4642 interferes with its interaction with intermediate filaments (Bouameur et al., 2013), and therefore, it is possible that plectin is phosphorylated at this residue in the central HD-like adhesions, which prevents its association with keratin filaments. Additionally, BP230, which is present in peripheral HDs but not central HD-like adhesions, may be required for efficient attachment of keratin filaments to the plasma membrane. In support of this supposition, BP230 knockout mice showed an impaired connection of keratin filaments with HDs (Guo et al., 1995). Similarly, reduced amounts of keratins are associated with type II HDs, which contain plectin but lack BP230 (Fontao et al., 1997; Uematsu et al., 1994).

Although an essential role of CD151 in the formation of type I HDs was not evident from our current experiments, a more subtle role of CD151 for the formation of HDs cannot be excluded. The ability of CD151 to facilitate the clustering of α3β1 and α6β4 into central HD-like adhesions may strengthen keratinocyte adhesion to newly deposited laminin-332 before FAs and HDs are fully established but once integrins are connected to the cytoskeleton, the function of CD151 as a clustering molecule may no longer be required. This model would indicate an important role of CD151-mediated adhesion strengthening and clustering of α3β1 and α6β4 into central HD-like adhesions *in vivo.* For example, during re-epithelization of wounded skin, when HDs are dissolved and stable adhesion of the keratinocytes to the basal lamina is no longer assured, the central HD-like adhesions may prevent detachment of migrating keratinocytes that are subject to external mechanical forces. At the same time, they may render the adhesion of keratinocytes sufficiently dynamic to allow integrin turnover and migration to occur. Consistent with a role of the central HD-like adhesions in migration, we found that these adhesions are more dynamic than the type I HDs.

Despite the fact that the association of BP230 with keratin filaments at type I HDs increases their stability (Michael et al., 2014; Seltmann et al., 2013), our FRAP analyses showed only a modest increase in the stability of the peripheral HD adhesions compared to the central HD-like adhesions. Since our FRAP analyses do not distinguish between peripheral adhesions that are or are not associated with keratin filaments, this apparent discrepancy may be explained by the notion that not all of the peripheral adhesions are associated with keratin filaments. Furthermore, it should be understood that the HD-like adhesions, unlike type I HDs, contain α3β1 and are connected to α6β4 through CD151. Thus, they will likely contribute to its stability, as well.

In central HD-like adhesions, CD151 and α3β1 colocalize, but in the periphery CD151 associates with type I HDs and α3β1 is localized into FAs. The localization of α3β1 into FAs coincides with the incorporation of BP230 in HDs. Since the localization of BP180 in type I HDs precedes that of BP230 (Koster et al., 2003), it is possible that BP180 displaces α3β1 from CD151 and allows the integrin to become incorporated into FAs. In this respect it is interesting to mention that, like CD151 and the integrin α3, α6 and β4 subunits (Yang et al., 2004), BP180 contains several cysteine residues adjacent to its transmembrane domain that are potential sites of palmitoylation. The role of protein palmitoylation in the formation of HDs is not known, but it is reasonable to suggest that it might help to increase the local concentration of HD proteins, and facilitate the assembly and stability of HDs.

In agreement with our finding that HDs can be formed in the absence of α3β1 in cultured keratinocytes, no obvious abnormalities in HDs have been observed in mice lacking integrin α3 in basal keratinocytes (Conti et al., 2003; DiPersio et al., 1997; Margadant et al., 2009). Yet, genetic ablation of the β1 integrin subunit or its co-activator kindlin-1 in basal keratinocytes has been associated with reduced HD protein expression and formation of HDs (Brakebusch et al., 2000; Qu et al., 2012; Raghavan et al., 2000). This suggests that if α3β1 has a role in HD formation, this role could be fulfilled by other integrins, as well. Furthermore, our finding that CD151 contributes to α3β1- but not α6β4-mediated strengthening of cell adhesions is consistent with the respective roles these proteins play in mediating cell-matrix adhesion in the skin and kidney. In the skin, where basal keratinocytes express both α3β1 and α6β4, the effect of CD151 deletion is relatively mild, and patients display only a mild skin blistering disorder. In contrast the loss of CD151 in glomerular podocytes, which express α3β1 but not α6β4, have been associated with progressive and irreversible kidney dysfunction (Crew et al., 2004; Kagan et al., 1988; Sachs et al., 2012; Vahidnezhad et al., 2017).

In conclusion, we show that CD151 stabilizes the central HD-like adhesions by strengthening the adhesion of α3β1 to laminin-332 and facilitating the incorporation of α6β4 into TEMs containing α3β1. On the other hand, CD151 is not needed for the formation or stabilization of α6β4-containing type I HDs in the periphery of the cells, which are linked to keratin filaments. These data provide new insights into the role of CD151 in the formation and maintenance of different populations of adhesions that are formed in cultured keratinocytes. Importantly, our study reflects the skin conditions, observed in CD151- and α3β1-mutant patients and mice and thus provides better understanding of the mechanisms underlying these conditions.

Material and methods

Antibodies

The primary and conjugated antibodies used in this study are listed in Table S1. Secondary antibodies for WB were goat anti-mouse IgG HRP (BioRad) and polyclonal goat anti-Rabbit IgG HRP (Dako). Donkey anti-mouse IgG PE (Jackson ImmunoResearch) was the secondary antibody used in FACS. For immunofluorescence (IF), rabbit anti-rat IgG (homemade), goat anti-guinea pig IgG Alexa Fluor (AF) 488, goat anti-human IgG AF488, goat anti-mouse AF568, goat anti-mouse AF647, goat anti-rabbit AF488, goat anti-rabbit AF647, goat anti-rat AF647 (Invitrogen), goat anti-mouse FITC, goat anti-rat FITC (Rockland) and the isotype specific goat anti-mouse IgG1 AF568 (ThermoFischer #A-21124) and goat anti-mouse IgG2a-FITC (Abcam #ab98697) were used secondary antibodies.

Cell lines

PA-JEB immortalized keratinocytes were isolated from a patient with Pyloric Atresia associated with Junctional Epidermolysis Bullosa (Niessen et al., 1996; Schaapveld et al., 1998). The derivation of this cell line was done for diagnostic purposes; thus, the research conducted using these cells was exempt of the requirement for ethical approval. PA-JEB/β4 keratinocytes stably expressing wild-type β4 were generated by retroviral transduction (Sterk et al., 2000) and maintained in serum-free keratinocyte medium (KGM; Invitrogen), supplemented with 50 µg ml^{-1} bovine pituitary gland extract, 5 ng ml^{-1} EGF, and antibiotics (100 units ml^{-1} streptomycin and 100 units ml^{-1} penicillin; Sigma). HaCaT keratinocytes, obtained from the American Type Culture Collection, were cultured in Dulbecco's modified Eagle's medium (DMEM; Gibco) containing 10% heat-inactivated fetal calf serum (FCS; Serana), and antibiotics. All cells were cultured at 37°C in a humidified, 5% CO_2 atmosphere.

The α3-, β4-, CD151- and plectin-deficient cells were prepared using CRISPR-Cas9 technology. Target sgRNAs against integrin α3 (5'-GCTACTCGGTCGCCCTCCAT-3'), integrin β4 (5'-GACTCGCTCCCTCCGCGCCT-3'), CD151 (5'-CAGGTTCCGACGCTCCTTGA-3') and plectin (5'-GAGGTGCTTGTTGACCCACT-3') were cloned into the pX330-U6-Chimeric_BB-CBh-hSpCas9 (Addgene plasmid #42230, deposited by Feng Zhang). For the α3-, β4- and CD151-deficient cells, cells were transiently transfected with this plasmid using lipofectamine® 2000 (Invitrogen) in OptiMEM (Gibco). The cells were bulk sorted for the population deficient of the protein of interest using a Moflo Asterios (Beckman Coulter) or FACSAria Fusion (BD Biosciences) cell sorter. For the preparation of the plectin-deficient cells, cells were cotransfected with a plasmid containing a blasticidin cassette flanked by TIA target sites (described by Blomen et al. 2015), blasticidin resistant cells were enriched by selection for four days in the presence of blasticidin (4 µg ml^{-1}; Sigma-Aldrich), clones were picked and analyzed for plectin expression by WB.

For (re)expression of proteins in protein deficient cells, we used stable cellular retroviral mediated transduction. Cells which expressed the protein were enriched by zeocin or blasticidin selection and/or by bulk sorting by FACS. The constructs used were: the β4-AD (D230A, P232A and E233A) in LZRS-IRES-blasticidin, a kind gift of Peter Marinkovich (Russell et al., 2003), the CD151 wt and CD151 palmitoylation mutant in LZRS-IRES-Zeo, constructed by introducing the CD151 cDNA released from pZeo-CD151 or pZeo-CD151-PALM (gift from F. Berditchevski (Berditchevski et al., 2002)) and the α3 wt in LZRS-IRES-Zeo. The α3 cDNA has been described previously (Delwel et al., 1994) and the full-length cDNA encoding human α3 was released from pUC18 by digesting with *Sph*I, made blunt by Klenow digestion and ligated into the *Swa*I site of the retroviral LZRS-IRES-zeo vector. Furthermore, the α3-G163A mutant in pBJ-1 expression vector (Zhang et al., 1999) was a gift from Yoshikazu Takada and transiently transfected in α3-deficient cells. Generation of PA-JEB keratinocytes stably expressing cells β4-RW (R1281W) has been described previously (Geerts et al., 1999).

Immunofluorescence imaging of fixed samples

For image acquisition, cells were seeded, at approximately 10-20% confluency, onto glass coverslips, uncoated or coated with 10 μg ml^{-1} fibronectin from bovine plasma (F1141, Sigma) and 5 μg ml^{-1} vitronectin (SRP3186, Sigma) and grown for 40-44 hours of which at least the last 20 hours in the presence of DMEM+FCS. After the cells had been fixed with 2% PFA for 10 min., permeabilized with 0.2% triton and blocked with 2% BSA (resolved in PBS; Serva), they were incubated for 50-60 minutes with primary and secondary antibodies, with three PBS washes in between. Nuclei were counterstained with DAPI (Sigma) and coverslips were mounted with MOWIOL for confocal imaging. For TIRF imaging coverslips were stored in PBS at 4°C until imaging.

Confocal imaging was performed using a Leica TCS SP5 confocal microscope with a 63x (NA 1.4) oil objective. A Leica SR-GSD microscope (Leica Microsystems, Wetzlar, Germany) equipped with a 160x oil immersion objective (NA 1.47) and an EMCCD Andor iXon camera (Andor Technology, Belfast, UK) was used to acquire TIRF images with an imaging depth of 200 nm. To be able to perform subsequent analyses, imaging was performed under equal conditions.

Image analyses were performed using ImageJ: Colocalization was assessed using Mander's overlap coefficient (MOC) with the JACoP plugin. The amount of basal cell surface clustering was quantified by calculating the integrated density of the staining. The intensity of the β4 staining in the peripheral adhesions was obtained by drawing a region of interest around the peripheral adhesions and measuring the mean intensity of the β4 staining in this region. The percentage of integrin β4 associated with plectin, BP230, keratin 14 or laminin-332 was obtained by calculating how much of the β4 positive area was additionally positive for plectin, BP230, keratin or laminin-332. The quantification of the island sizes was performed by thresholding images based on their staining with Phalloidin-

iFluor647 (AAT Bioquest) and measuring the surface area after selecting the outer region. Furthermore, the quantification of the amount of central β4 clusters present per cell island was performed using an arbitrary scoring system (0 = no central adhesions, 1 = few central adhesions, 2 = several central adhesions, 3 = many central adhesions).

Graphs were made using GraphPad Prism and include bar graphs showing the mean and accompanied standard deviation (including dots that represent independent measurement) or boxplots dividing the data in quartiles. The number of images used for analyses is specified in the figure legends and statistical significance was calculated using the non-parametric and non-paired Mann-Whitney U test; P values: * < 0.05, ** < 0.01, *** < 0.001, ****< 0.0001.

Live imaging and FRAP

For live imaging and Fluorescence Recovery After Photobleaching (FRAP), cells were seeded on 24 mm coverslips and imaging was performed using a Leica TCS SP5 confocal microscope with a 63x (NA 1.4) oil objective equipped with a live cell chamber. Live imaging of CD151-proficient and -deficient PA-JEB/β4GFP cells was started 20h after seeding and immediately after replacing the KGM medium by DMEM+FCS. Every hour the differential interference contrast (DIC) and GFP fluorescent signals were collected of multiple cell islands at different positions. Videos were made in ImageJ.

FRAP experiments were performed, using the FRAP wizard in LAS-AF, using PA-JEB/β4GFP cells grown for 20h in KGM medium and subsequently grown for an additional 20h in DMEM+FCS. Simultaneously a region in one peripheral- and one central-α6β4 containing adhesion was bleached and fluorescent recovery was followed over time. Two images as controls were taken before bleaching and then 1 image every 10 (first 2 minutes) or 30 seconds for 15 minutes after bleaching. For analyses, the background was subtracted from the measured intensities and the curves where normalized to the mean value before bleaching. Furthermore, the values of the first 230 seconds were fitted with a single exponential decay using MATLAB software and the fitted curve was used to calculate the mobile fraction and the recovery time τ. Graphs are made using GraphPad Prism; the line plot shows the mean with standard deviations and the boxplots divide the data in quartiles. The number of images used for analyses is specified in the figure legends and the significance difference between the central and peripheral adhesions was calculated using the non-parametric Wilcoxon matched-pairs signed rank test (at different time points); P values: ** < 0.01, *** < 0.001.

Flow Cytometry/FACS

For FACS analyses, cells were collected after trypsinization, and incubated for 50-60 min with primary and secondary antibodies on ice in PBS containing 2% FCS. In between the antibody steps, cells were washed twice with 2% FCS in PBS. Finally, cells were passed through a nylon mesh filter and 50000+ cells were analyzed per sample using a FACSCalibur cell analyzer (BD Biosciences). Cells incubated with only secondary antibody were used as a negative control. Graphs include values of a representative experiment (out of three repetitions) normalized to the mode. The graphs were made in FlowJo and adapted in Adobe Illustrator®.

Adhesion strengthening assay

To measure long-term adhesion strength of cells, we used the spinning disk assay described by Boettiger (Boettiger, 2007). Wild-type or KO HaCaT cells were grown to 60-100% confluence on 30 mm coverslips for two days. Just before spinning, the cells were washed briefly with PBS and the coverslips were 'glued' to the stamp using grease. The cells were spun for 8 min at 4240 rpm in PBS-ABC buffer (80% A (10 gL^{-1} NaCL, 0.25 gL^{-1} KCL, 0.95 gL^{-1} $Na_2HPO_4*2H_2$, 0.25 gL^{-1} KH_2PO_4), 10% B (1.34 gL^{-1} $CaCl_2.2H_2O$) and 10% C (2 gL^{-1} $MgCl_2.6H_2O$)) containing 5% dextran from Leuconostoc Spp. Mr 450,000-600,000 (Sigma). After spinning, the cells were fixed in 2% PFA, permeabilized in 0.2% triton-X100, stained with DAPI and mounted on microscopic slides using MOWIOL. The complete coverslips were imaged using a Zeiss AxioObserver Z1. The coverslip area was divided in rings with a 1.5 mm diameter and the cell confluency was measured per ring and normalized to the total area of the ring and to the confluency in the middle area (100% confluent). The average shear stress per ring was calculated using the formula $\tau = 10 * (0{,}8\, r \sqrt{\rho\mu\omega^3})$ with τ is the shear stress in dynes/cm^2, r is the radial distance from the center of rotation in m, ρ is the fluid density in kg m^{-3}, μ is the fluid viscosity in Pa*s and ω is the rotational velocity in radians per minute. The τ50 was obtained by fitting the data points to a logistic function $f = \frac{100}{1+\exp[(\tau-c)/b]}$ using MATLAB software with c is the inflection point and equal to the point of 50% cell detachment (τ50) and b is the slope at the inflection point.

Graphs were generated and significance was calculated using GraphPad Prism. The line plots show the mean value of the 9-16 experiments per condition, which are individually shown as squares, diamonds or triangles. For the WT line, the same dataset was used in the different graphs. The significance of the percentage of adherent cells in KO cells compared to the WT cells was calculated at each data point using unpaired T-tests corrected for multiple comparisons using the Holm-Sidak method; p values: *** < 0.001, ****< 0.0001. The τ50 was visualized in a bar graph showing the mean with standard deviation of 9-10 independent experiments. The significant different between the τ50 in β4 KO and β4+CD151 KO cells was calculated using the non-parametric Mann-Whitney U test; P value: ****< 0.0001.

Immunoprecipitations and western blot

For analysis of proteins in whole cell lysates, subconfluent cells were washed in cold PBS, lysed in RIPA (1% NP-40, 0.5% sodium deoxycholate, 0.1% SDS, 4 mM EDTA (pH 7.5), 100 mM NaCl, 20 mM Tris-HCl (pH 7.5)) supplemented with inhibitors (1.5 mM Na3VO4, 15 mM NaF and protease inhibitor cocktail (1:500)), whole cell lysates were cleared by centrifugation at 12000 rpm for 60 min at 4°C and supplemented with SDS sample buffer (50 mM Tris-HCl pH 6.8, 2% SDS, 10% glycerol, 12.5 mM EDTA, 0.02% Bromophenol Blue) with or without β-mercaptoethanol and heated at 95°C for 5 min. Immunoprecipitations were performed with cell lysates prepared in 1% NonidetP-40, 100 mM NaCl, 4 mM EDTA, 20 mM Tris-HCl (pH 7.5), supplemented with inhibitors. After centrifugation at 12.000 rpm for 60 min at 4°C, the cleared lysates were incubated at 4°C for 1.5h with 1 µg ml^{-1} antibody. Subsequently, the lysates were incubated overnight with Protein G Sepharose 4 Fast Flow beads (GE Healthcare), beads were washed three times with lysis buffer and two times with PBS and bound proteins were dissolved in SDS sample buffer without β-mercaptoethanol and heated at 95°C for 5 min.

Proteins were separated on 4-12% bolt Novex gradient gels (Invitrogen) and transferred to Immobilon-P transfer membranes (Millipore). The membrane was blocked for at least 2.5 h in 2% BSA in TBST (10 mM Tris (pH 7.5), 150 mM NaCl, 0.05% Tween 20) before incubation with primary antibody overnight at 4°C and with secondary antibody for 1h at room temperature. After each incubation, membranes were washed twice with TBST and twice with TBS (TBST without Tween 20). Antibodies were detected using Clarity Western ECL Substrate (Bio-Rad) and in the figures the molecular weight markers (kDa) are indicated.

Acknowledgements

We thank Leila Nahidiazar, Bram van den Broek, Lenny Brocks and Marjolijn Mertz for their help with imaging and image analysis; Martijn van Baalen, Anita Pfauth, Frank van Diepen and Debajit Bhowmick for their help with cell sorting; Patrick Celie for conjugating Alexa488 to the J143 antibody and Alba Zuidema, Veronika Ramovs, Jose de Pereda and Kevin Wilhelmsen for critical reading of the manuscript. Furthermore, we thank our colleagues for sharing reagents.

Competing interests

The authors declare no competing interests.

Author contributions

Conceptualization: L.t.M., A.S.; Methodology: L.t.M., J.J., W.W., M.K.; Software: R.H.; Verification: L.t.M.; Analysis: L.t.M., R.H.; Investigation: L.t.M., J.J.; Writing-original draft: L.t.M., A.S.; Writing-review and editing: L.t.M., R.H., W.W., A.S.; Visualization: L.t.M.; Supervision: A.S.

Funding

This work was supported by grants from the Netherlands Organization for Scientific Research (NWO; project number 824.14.010), the Dutch Cancer Society (project number 2013-5971) and by a grant from NWO as part of the National Roadmap Large-scale Research Facilities of the Netherlands, Proteins@Work (project number 184.032.201).

Data availability

All relevant data are available from the authors on reasonable request.

List of abbreviations

ECM, extracellular matrix; HD, hemidesmosome; EB, epidermolysis bullosa; FA, focal adhesion; TEM, tetraspanin enriched micro domain; WT, wild-type; KO, knock-out; MUT, mutant; RESC, rescue; WB, Western blot; IP, immunoprecipitation; FACS, fluorescence activated cell sorting; TIRF, total internal reflection fluorescence; IF, immune fluorescence; MOC, Mander's overlap coefficient; DAPI, 4',6-diamidino-2-phenylindole; FRAP, fluorescent recovery after photobleaching.

References

Andrä, K., Lassmann, H., Bittner, R., Shorny, S., Fässler, R., Propst, F., Wiche, G. (1997). Targeted inactivation of plectin reveals essential function in maintaining the integrity of skin, muscle, and heart cytoarchitecture. Genes Dev. 11, 3143–3156.

Ashton, G.H., Sorelli, P., Mellerio, J.E., Keane, F.M., Eady, R.A., McGrath, J.A. (2001). Alpha 6 beta 4 integrin abnormalities in junctional epidermolysis bullosa with pyloric atresia. Br. J. Dermatol. 144, 408–414.

Berditchevski, F. (2001). Complexes of tetraspanins with integrins: more than meets the eye. J. Cell Sci. 114, 4143–4151.

Berditchevski, F., Odintsova, E., Sawada, S., Gilbert, E. (2002). Expression of the palmitoylation-deficient CD151 weakens the association of alpha 3 beta 1 integrin with the tetraspanin-enriched microdomains and affects integrin-dependent signaling. J. Biol. Chem. 277, 36991–37000. https://doi.org/10.1074/jbc.M205265200

Blomen, V.A., Májek, P., Jae, L.T., Bigenzahn, J.W., Nieuwenhuis, J., Staring, J., Sacco, R., van Diemen, F.R., Olk, N., Stukalov, A., Marceau, C., Janssen, H., Carette, J.E., Bennett, K.L., Colinge, J., Superti-Furga, G., Brummelkamp, T.R. (2015). Gene essentiality and synthetic lethality in haploid human cells. Science 350, 1092–1096. https://doi.org/10.1126/science.aac7557

Boettiger, D. (2007). Quantitative measurements of integrin-mediated adhesion to extracellular matrix. Meth. Enzymol. 426, 1–25. https://doi.org/10.1016/S0076-6879(07)26001-X

Bouameur, J.-E., Schneider, Y., Begré, N., Hobbs, R.P., Lingasamy, P., Fontao, L., Green, K.J., Favre, B., Borradori, L. (2013). Phosphorylation of serine 4,642 in the C-terminus of plectin by MNK2 and PKA modulates its interaction with intermediate filaments. J. Cell Sci. 126, 4195–4207. https://doi.org/10.1242/jcs.127779

Brakebusch, C., Grose, R., Quondamatteo, F., Ramirez, A., Jorcano, J.L., Pirro, A., Svensson, M., Herken, R., Sasaki, T., Timpl, R., Werner, S., Fässler, R. (2000). Skin and hair follicle integrity is crucially dependent on beta 1 integrin expression on keratinocytes. EMBO J. 19, 3990–4003. https://doi.org/10.1093/emboj/19.15.3990

Conti, F.J.A., Rudling, R.J., Robson, A., Hodivala-Dilke, K.M. (2003). alpha3beta1-integrin regulates hair follicle but not interfollicular morphogenesis in adult epidermis. J. Cell Sci. 116, 2737–2747. https://doi.org/10.1242/jcs.00475

Crew, V.K., Burton, N., Kagan, A., Green, C.A., Levene, C., Flinter, F., Brady, R.L., Daniels, G., Anstee, D.J. (2004). CD151, the first member of the tetraspanin (TM4) superfamily detected on erythrocytes, is essential for the correct assembly of human basement membranes in kidney and skin. Blood 104, 2217–2223. https://doi.org/10.1182/blood-2004-04-1512

Delwel, G.O., de Melker, A.A., Hogervorst, F., Jaspars, L.H., Fles, D.L., Kuikman, I., Lindblom, A., Paulsson, M., Timpl, R., Sonnenberg, A. (1994). Distinct and overlapping ligand specificities of the alpha 3A beta 1 and alpha 6A beta 1 integrins: recognition of laminin isoforms. Mol. Biol. Cell 5, 203–215.

DiPersio, C.M., Hodivala-Dilke, K.M., Jaenisch, R., Kreidberg, J.A., Hynes, R.O. (1997). alpha3beta1 Integrin is required for normal development of the epidermal basement membrane. J. Cell Biol. 137, 729–742.

Dowling, J., Yu, Q.C., Fuchs, E. (1996). Beta4 integrin is required for hemidesmosome formation, cell adhesion and cell survival. J. Cell Biol. 134, 559–572.

Fontao, L., Dirrig, S., Owaribe, K., Kedinger, M., Launay, J.F. (1997). Polarized expression of HD1: relationship with the cytoskeleton in cultured human colonic carcinoma cells. Exp. Cell Res. 231, 319–327. https://doi.org/10.1006/excr.1996.3465

Geerts, D., Fontao, L., Nievers, M.G., Schaapveld, R.Q., Purkis, P.E., Wheeler, G.N., Lane, E.B., Leigh, I.M., Sonnenberg, A. (1999). Binding of integrin alpha6beta4 to plectin prevents plectin association with F-actin but does not interfere with intermediate filament binding. J. Cell Biol. 147, 417–434.

Geuijen, C.A.W., Sonnenberg, A. (2002). Dynamics of the alpha6beta4 integrin in keratinocytes. Mol. Biol. Cell 13, 3845–3858. https://doi.org/10.1091/mbc.02-01-0601

Groves, R.W., Liu, L., Dopping-Hepenstal, P.J., Markus, H.S., Lovell, P.A., Ozoemena, L., Lai-Cheong, J.E., Gawler, J., Owaribe, K., Hashimoto, T., Mellerio, J.E., Mee, J.B., McGrath, J.A. (2010). A homozygous nonsense mutation within the dystonin gene coding for the coiled-coil domain of the epithelial isoform of BPAG1 underlies a new subtype of autosomal recessive epidermolysis bullosa simplex. J. Invest. Dermatol. 130, 1551–1557. https://doi.org/10.1038/jid.2010.19

Guo, L., Degenstein, L., Dowling, J., Yu, Q.-C., Wollmann, R., Perman, B., Fuchs, E. (1995). Gene targeting of BPAG1: Abnormalities in mechanical strength and cell migration in stratified epithelia and neurologic degeneration. Cell 81, 233–243. https://doi.org/10.1016/0092-8674(95)90333-X

Has, C., Fischer, J. (2018). Inherited epidermolysis bullosa: New diagnostics and new clinical phenotypes. Exp. Dermatol. 1-7. https://doi.org/10.1111/exd.13668

Has, C., Spartà, G., Kiritsi, D., Weibel, L., Moeller, A., Vega-Warner, V., Waters, A., He, Y., Anikster, Y., Esser, P., Straub, B.K., Hausser, I., Bockenhauer, D., Dekel, B., Hildebrandt, F., Bruckner-Tuderman, L., Laube, G.F. (2012). Integrin α3 mutations with kidney, lung, and skin disease. N. Engl. J. Med. 366, 1508–1514. https://doi.org/10.1056/NEJMoa1110813

Hemler, M.E. (2005). Tetraspanin functions and associated microdomains. Nat. Rev. Mol. Cell Biol. 6, 801–811. https://doi.org/10.1038/nrm1736

Jonkman, M.F., de Jong, M.C., Heeres, K., Pas, H.H., van der Meer, J.B., Owaribe, K., Martinez de Velasco, A.M., Niessen, C.M., Sonnenberg, A. (1995). 180-kD bullous pemphigoid antigen (BP180) is deficient in generalized atrophic benign epidermolysis bullosa. J. Clin. Invest. 95, 1345–1352. https://doi.org/10.1172/JCI117785

Kagan, A., Feld, S., Chemke, J., Bar-Khayim, Y. (1988). Occurrence of hereditary nephritis, pretibial epidermolysis bullosa and beta-thalassemia minor in two siblings with end-stage renal disease. Nephron 49, 331–332. https://doi.org/10.1159/000185086

Koster, J., Geerts, D., Favre, B., Borradori, L., Sonnenberg, A. (2003). Analysis of the interactions between BP180, BP230, plectin and the integrin alpha6beta4 important for hemidesmosome assembly. J. Cell Sci. 116, 387–399.

Litjens, S.H.M., de Pereda, J.M., Sonnenberg, A. (2006). Current insights into the formation and breakdown of hemidesmosomes. Trends Cell Biol. 16, 376–383. https://doi.org/10.1016/j.tcb.2006.05.004

Liu, L., Dopping-Hepenstal, P.J., Lovell, P.A., Michael, M., Horn, H., Fong, K., Lai-Cheong, J.E., Mellerio, J.E., Parsons, M., McGrath, J.A. (2012). Autosomal recessive epidermolysis bullosa simplex due to loss of BPAG1-e expression. J. Invest. Dermatol. 132, 742–744. https://doi.org/10.1038/jid.2011.379

Margadant, C., Raymond, K., Kreft, M., Sachs, N., Janssen, H., Sonnenberg, A. (2009). Integrin α3β1 inhibits directional migration and wound re-epithelialization in the skin. J. Cell Sci. 122, 278–288. https://doi.org/10.1242/jcs.029108

McLean, W.H., Pulkkinen, L., Smith, F.J., Rugg, E.L., Lane, E.B., Bullrich, F., Burgeson, R.E., Amano, S., Hudson, D.L., Owaribe, K., McGrath, J.A., McMillan, J.R., Eady, R.A., Leigh, I.M., Christiano, A.M., Uitto, J. (1996). Loss of plectin causes epidermolysis bullosa with muscular dystrophy: cDNA cloning and genomic organization. Genes Dev. 10, 1724–1735.

McMillan, J.R., McGrath, J.A., Tidman, M.J., Eady, R.A. (1998). Hemidesmosomes show abnormal association with the keratin filament network in junctional forms of epidermolysis bullosa. J. Invest. Dermatol. 110, 132–137. https://doi.org/10.1046/j.1523-1747.1998.00102.x

Michael, M., Begum, R., Fong, K., Pourreyron, C., South, A.P., McGrath, J.A., Parsons, M. (2014). BPAG1-e restricts keratinocyte migration through control of adhesion stability. J. Invest. Dermatol. 134, 773–782. https://doi.org/10.1038/jid.2013.382

Nakamura, H., Sawamura, D., Goto, M., Nakamura, H., McMillan, J.R., Park, S., Kono, S., Hasegawa, S., Paku, S., Nakamura, T., Ogiso, Y., Shimizu, H. (2005). Epidermolysis bullosa simplex associated with pyloric atresia is a novel clinical subtype caused by mutations in the plectin gene (PLEC1). J. Mol. Diagn. 7, 28–35. https://doi.org/10.1016/S1525-1578(10)60005-0

Niessen, C.M., van der Raaij-Helmer, M.H., Hulsman, E.H., van der Neut, R., Jonkman, M.F., Sonnenberg, A. (1996). Deficiency of the integrin beta 4 subunit in junctional epidermolysis bullosa with pyloric atresia: consequences for hemidesmosome formation and adhesion properties. J. Cell Sci. 109 (Pt 7), 1695–1706.

Nievers, M.G., Kuikman, I., Geerts, D., Leigh, I.M., Sonnenberg, A. (2000). Formation of hemidesmosome-like structures in the absence of ligand binding by the (alpha)6(beta)4 integrin requires binding of HD1/plectin to the cytoplasmic domain of the (beta)4 integrin subunit. J. Cell Sci. 113 (Pt 6), 963–973.

Puklin-Faucher, E., Sheetz, M.P. (2009). The mechanical integrin cycle. J. Cell Sci. 122, 179–186. https://doi.org/10.1242/jcs.042127

Qu, H., Wen, T., Pesch, M., Aumailley, M. (2012). Partial loss of epithelial phenotype in kindlin-1-deficient keratinocytes. Am. J. Pathol. 180, 1581–1592. https://doi.org/10.1016/j.ajpath.2012.01.005

Raghavan, S., Bauer, C., Mundschau, G., Li, Q., Fuchs, E. (2000). Conditional ablation of beta1 integrin in skin. Severe defects in epidermal proliferation, basement membrane formation, and hair follicle invagination. J. Cell Biol. 150, 1149–1160.

Russell, A.J., Fincher, E.F., Millman, L., Smith, R., Vela, V., Waterman, E.A., Dey, C.N., Guide, S., Weaver, V.M., Marinkovich, M.P. (2003). Alpha 6 beta 4 integrin regulates keratinocyte chemotaxis through differential GTPase activation and antagonism of alpha 3 beta 1 integrin. J. Cell Sci. 116, 3543–3556. https://doi.org/10.1242/jcs.00663

Sachs, N., Kreft, M., van den Bergh Weerman, M.A., Beynon, A.J., Peters, T.A., Weening, J.J., Sonnenberg, A. (2006). Kidney failure in mice lacking the tetraspanin CD151. J. Cell Biol. 175, 33–39. https://doi.org/10.1083/jcb.200603073

Sachs, N., Secades, P., Hulst, L. van, Kreft, M., Song, J.-Y., Sonnenberg, A. (2012). Loss of integrin α3 prevents skin tumor formation by promoting epidermal turnover and depletion of slow-cycling cells. PNAS *USA* 109, 21468–21473. https://doi.org/10.1073/pnas.1204614110

Schaapveld, R.Q., Borradori, L., Geerts, D., van Leusden, M.R., Kuikman, I., Nievers, M.G., Niessen, C.M., Steenbergen, R.D., Snijders, P.J., Sonnenberg, A. (1998). Hemidesmosome formation is initiated by the beta4 integrin subunit, requires complex formation of beta4 and HD1/plectin, and involves a direct interaction between beta4 and the bullous pemphigoid antigen 180. J. Cell Biol. 142, 271–284.

Seltmann, K., Roth, W., Kröger, C., Loschke, F., Lederer, M., Hüttelmaier, S., Magin, T.M. (2013). Keratins mediate localization of hemidesmosomes and repress cell motility. J. Invest. Dermatol. 133, 181–190. https://doi.org/10.1038/jid.2012.256

Sincock, P.M., Mayrhofer, G., Ashman, L.K. (1997). Localization of the transmembrane 4 superfamily (TM4SF) member PETA-3 (CD151) in normal human tissues: comparison with CD9, CD63, and alpha5beta1 integrin. J. Histochem. Cytochem. 45, 515–525. https://doi.org/10.1177/002215549704500404

Sonnenberg, A., Calafat, J., Janssen, H., Daams, H., van der Raaij-Helmer, L.M.H., Falcioni, R., Kennel, S.J., Aplin, J.D., Baker, J., Loizidou, M., Garrod, D. (1991). Integrin alpha 6/beta 4 complex is located in hemidesmosomes, suggesting a major role in epidermal cell-basement membrane adhesion. J. Cell Biol. 113, 907–917.

Sterk, L.M., Geuijen, C.A., Oomen, L.C., Calafat, J., Janssen, H., Sonnenberg, A. (2000). The tetraspan molecule CD151, a novel constituent of hemidesmosomes, associates with the integrin alpha6beta4 and may regulate the spatial organization of hemidesmosomes. J. Cell Biol. 149, 969–982.

Sterk, L.M.T., Geuijen, C.A.W., Berg, J.G. van den, Claessen, N., Weening, J.J., Sonnenberg, A. (2002). Association of the tetraspanin CD151 with the laminin-binding integrinsα 3β1, α6β1, α6β4 and α7β1 in cells in culture and in vivo. J. Cell Sci. 115, 1161–1173.

Stipp, C.S. (2010). Laminin-binding integrins and their tetraspanin partners as potential antimetastatic targets. Expert Rev. Mol. Med. 12. https://doi.org/10.1017/S1462399409001355

Termini, C.M., Gillette, J.M. (2017). Tetraspanins Function as Regulators of Cellular Signaling. Front Cell Dev. Biol. 5, 34. https://doi.org/10.3389/fcell.2017.00034

Uematsu, J., Nishizawa, Y., Sonnenberg, A., Owaribe, K. (1994). Demonstration of type II hemidesmosomes in a mammary gland epithelial cell line, BMGE-H. J. Biochem. 115, 469–476.

Underwood, R.A., Carter, W.G., Usui, M.L., Olerud, J.E. (2009). Ultrastructural Localization of Integrin Subunits β4 and α3 Within the Migrating Epithelial Tongue of In Vivo Human Wounds. J. Histochem. Cytochem. 57, 123–142. https://doi.org/10.1369/jhc.2008.952176

Vahidnezhad, H., Youssefian, L., Saeidian, A.H., Mahmoudi, H.R., Touati, A., Abiri, M., Kajbafzadeh, A.-M., Aristodemou, S., Liu, L., McGrath, J.A., Ertel, A., Londin, E., Kariminejad, A., Zeinali, S., Fortina, P., Uitto, J. (2017). Recessive mutation in tetraspanin CD151 causes Kindler syndrome-like epidermolysis bullosa with multi-systemic manifestations including nephropathy. Matrix Biol. https://doi.org/10.1016/j.matbio.2017.11.003

van der Neut, R., Krimpenfort, P., Calafat, J., Niessen, C.M., Sonnenberg, A. (1996). Epithelial detachment due to absence of hemidesmosomes in integrin β4 null mice. Nat. Genet. 13, 366–369. https://doi.org/10.1038/ng0796-366

Vidal, F., Aberdam, D., Miquel, C., Christiano, A.M., Pulkkinen, L., Uitto, J., Ortonne, J.P., Meneguzzi, G. (1995). Integrin beta 4 mutations associated with junctional epidermolysis bullosa with pyloric atresia. Nat. Genet. 10, 229–234. https://doi.org/10.1038/ng0695-229

Walko, G., Castañón, M.J., Wiche, G. (2015). Molecular architecture and function of the hemidesmosome. Cell Tissue Res. https://doi.org/10.1007/s00441-015-2216-6

Wright, M.D., Geary, S.M., Fitter, S., Moseley, G.W., Lau, L.-M., Sheng, K.-C., Apostolopoulos, V., Stanley, E.G., Jackson, D.E., Ashman, L.K. (2004). Characterization of Mice Lacking the Tetraspanin Superfamily Member CD151. Mol. Cell Biol. 24, 5978–5988. https://doi.org/10.1128/MCB.24.13.5978-5988.2004

Yang, X., Claas, C., Kraeft, S.-K., Chen, L.B., Wang, Z., Kreidberg, J.A., Hemler, M.E. (2002). Palmitoylation of Tetraspanin Proteins: Modulation of CD151 Lateral Interactions, Subcellular Distribution, and Integrin-dependent Cell Morphology. Mol. Biol. Cell 13, 767–781. https://doi.org/10.1091/mbc.01-05-0275

Yang, X., Kovalenko, O.V., Tang, W., Claas, C., Stipp, C.S., Hemler, M.E. (2004). Palmitoylation supports assembly and function of integrin-tetraspanin complexes. J. Cell Biol. 167, 1231–1240. https://doi.org/10.1083/jcb.200404100

Zhang, X.P., Puzon-McLaughlin, W., Irie, A., Kovach, N., Prokopishyn, N.L., Laferté, S., Takeuchi, K., Tsuji, T., Takada, Y. (1999). Alpha 3 beta 1 adhesion to laminin-5 and invasin: critical and differential role of integrin residues clustered at the boundary between alpha 3 N-terminal repeats 2 and 3. Biochemistry 38, 14424–14431.

Figures

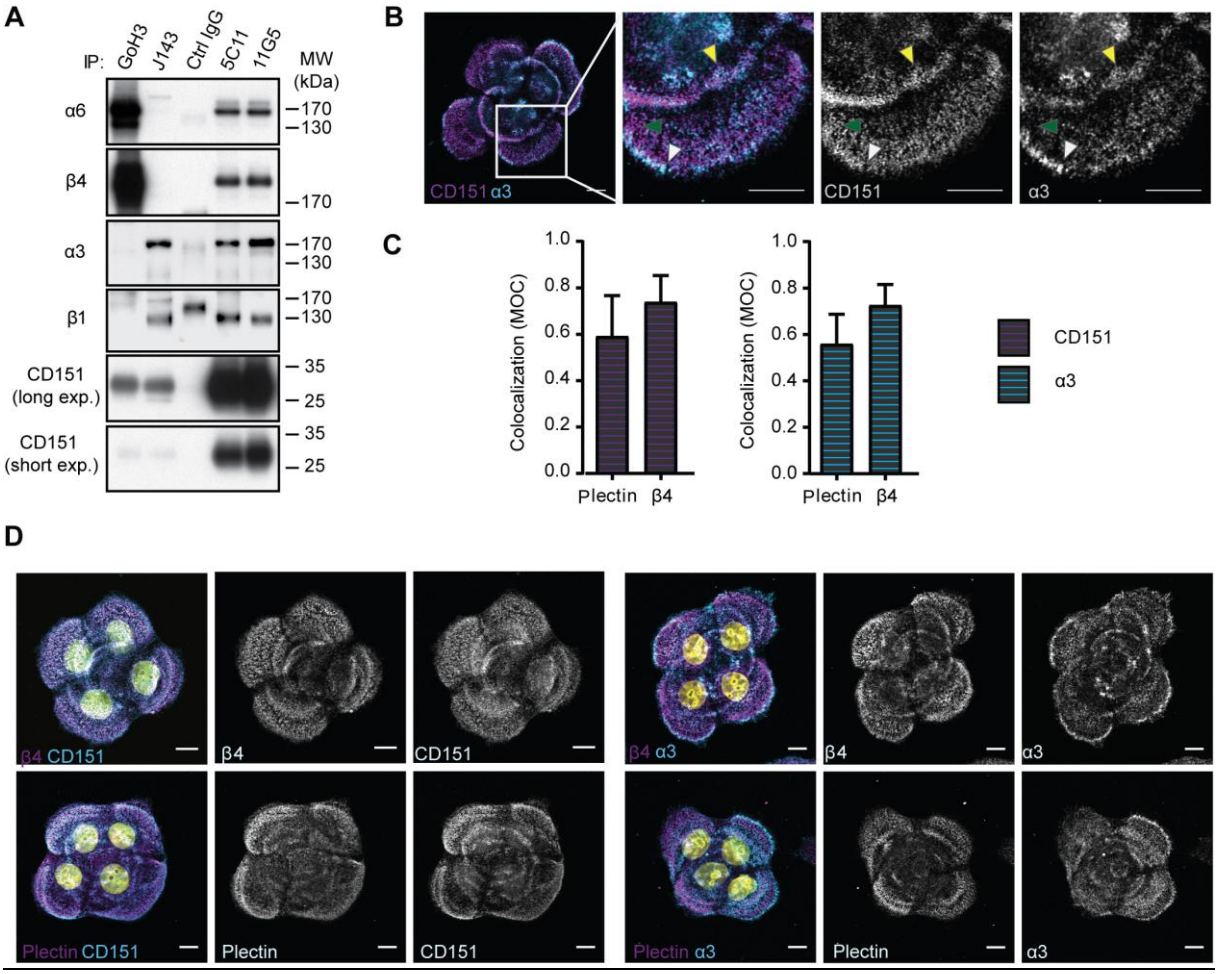

Fig. 1. Association of CD151 with α3β1 and α6β4 in adhesion complexes.

(A) Detection of α3β1-CD151 and α6β4-CD151 complexes in lysates of PA-JEB/β4 keratinocytes using immunoprecipitation and Western Blotting under nonreducing conditions. Antibodies used for immunoprecipitation were GoH3 against α6, J143 against α3, and 5C11 and 11G5 against CD151. (B) Confocal overview and zoom-in image of PA-JEB/β4 cells stained for α3 (cyan) and CD151 (magenta). Yellow arrow heads indicate adhesions containing α3 and CD151 and white and dark green arrow heads indicate α3 and CD151 located independently of each other in the periphery of the cells. Scale bars are 10 µm. (C) Quantification of the colocalization (MOC) of α3 (46 images from 2 independent experiments (exp.)) or CD151 (30 images; 2 exp.) with plectin and α3 (52 images; 2 exp.) or CD151 (74 images; 4 exp.) with β4. (D) Confocal images of double-IF staining of CD151, α3 (cyan) and HD components plectin and β4 (magenta) in PA-JEB/β4 keratinocytes. Nuclei were counterstained with DAPI (yellow) and scale bars are 10 µm.

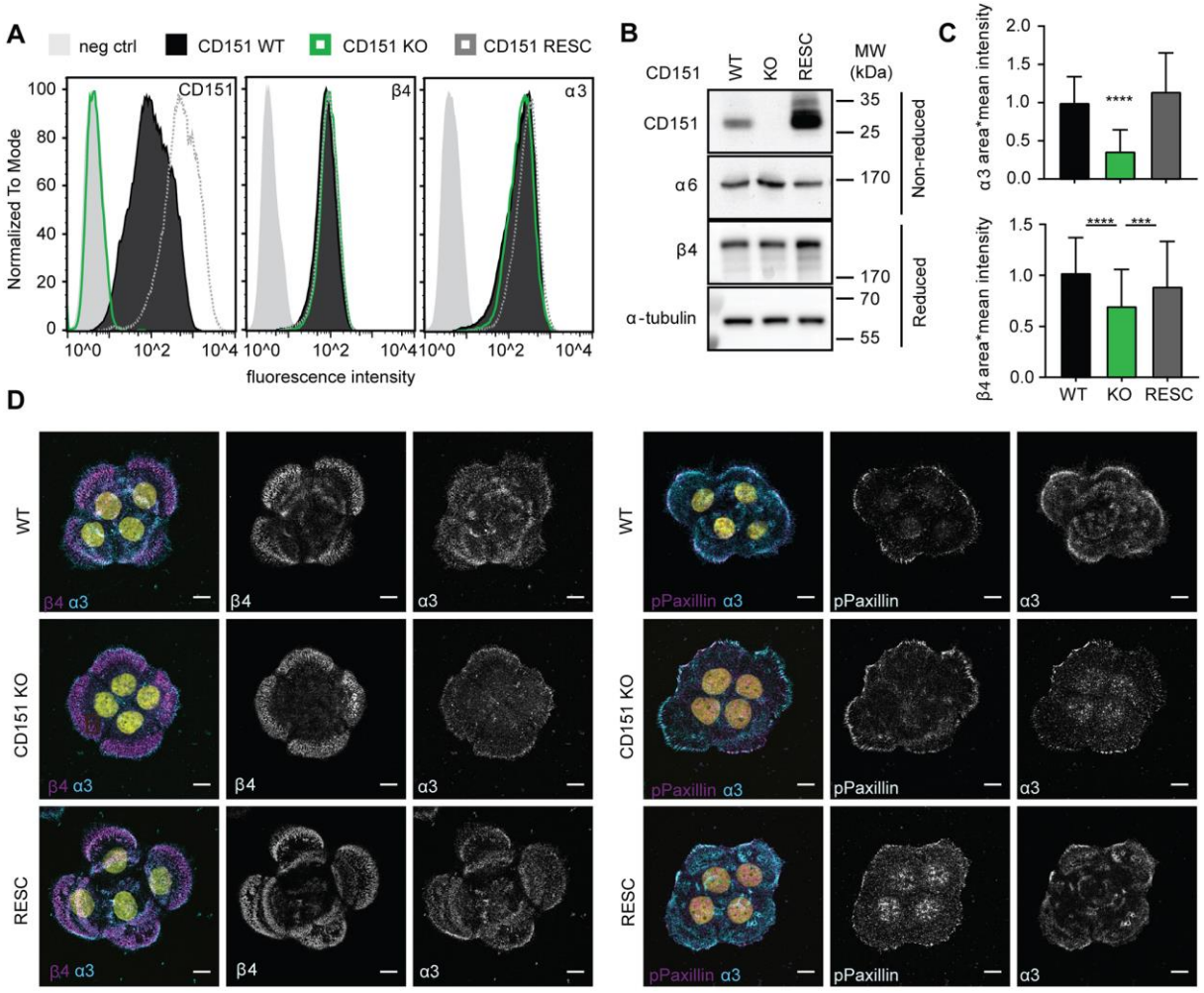

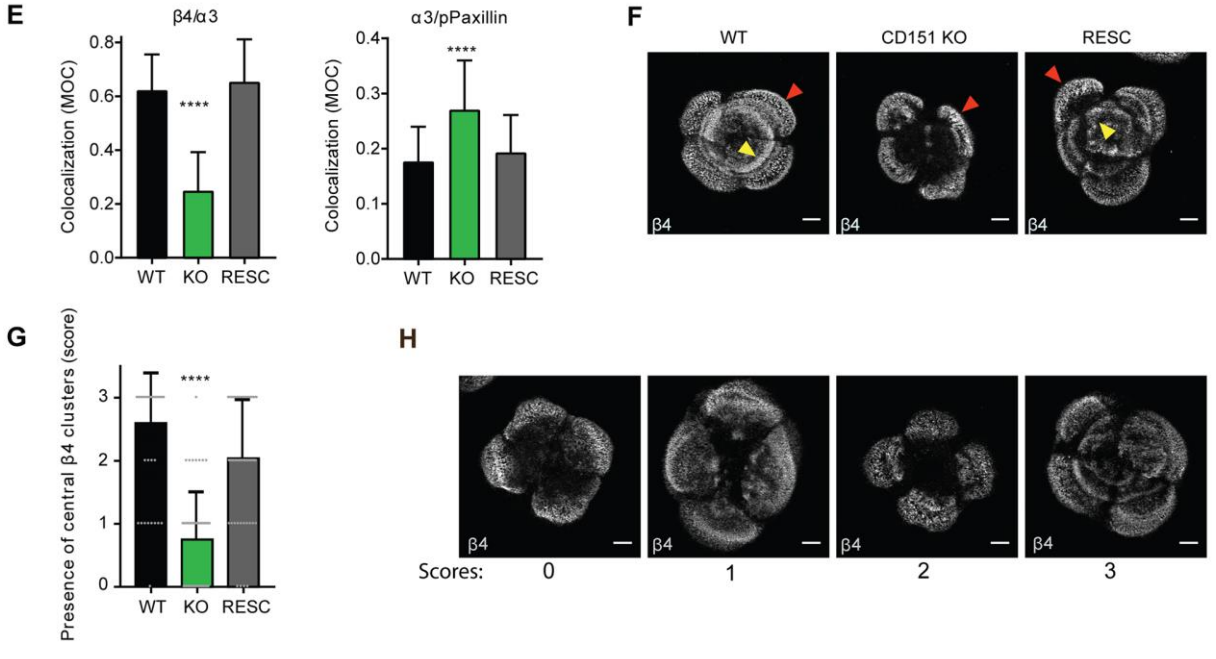

Fig. 2. CD151 influences localization of adhesions containing α3β1 and α6β4.

(A) FACS analysis of surface expression of CD151, β4 and α3 for CD151-WT, -KO and -RESC PA-JEB/β4 cells. (B) Whole cell lysate of WT, CD151-KO and CD151-RESC PA-JEB/β4 keratinocytes analyzed by WB for protein levels of CD151, α6, β4 and α-tubulin (loading control) under reduced or non-reduced conditions as indicated. (C) Quantification of the amount of α3 (WT: 55, KO: 57 and RESC: 55 images; 3 exp. each) and β4 (WT: 122, KO: 122 and RESC: 119 images; 8 exp. each) clustering at the basal cell surface (α3 or β4 area*intensity). Graph: Mean+s.d.; P values: ***< 0.001, ****< 0.0001 (Mann-Whitney U test). (D) Confocal images of WT, CD151-KO and CD151-RESC PA-JEB/β4 keratinocytes stained for α3 (cyan) and β4 (magenta), or α3 (cyan) and phosphorylated paxillin (magenta). Nuclei were counterstained with DAPI (yellow). Scale bars are 10 µm (E) Quantification of the colocalization (MOC) of β4 and α3 (WT: 56, KO: 55 and RESC: 57 images; 3 exp. each) and of α3 and phosphorylated paxillin (WT: 55, KO: 57 and RESC: 55 images; 3 exp. each). Graph: Mean+s.d.; P value: ****< 0.0001 (Mann-Whitney U test). (F) Confocal images of WT and CD151-KO and CD151-RESC PA-JEB/β4 keratinocytes stained for β4. Red arrowheads show peripheral α6β4-containing adhesions, while yellow arrowheads point to central α6β4-containing adhesions. Scale bars are 10 µm. (G) Quantification of the amount of central α6β4-containing adhesions per cell island (dots represent individual cell islands) using images from WT (57 images; 4 exp.), CD151-KO (56 images; 4 exp.) and CD151-RESC (55 images; 4 exp.) PA-JEB/β4 cells stained for β4. Graph: Mean+s.d.; P value: ****< 0.0001 (Mann-Whitney U test). (H) Scoring system for the amount of central α6β4-containing adhesions present, with example images. 0 = no central adhesion, 1 = little central adhesions, 2 = several central adhesions, 3 = many central adhesions. Scale bars are 10 µm.

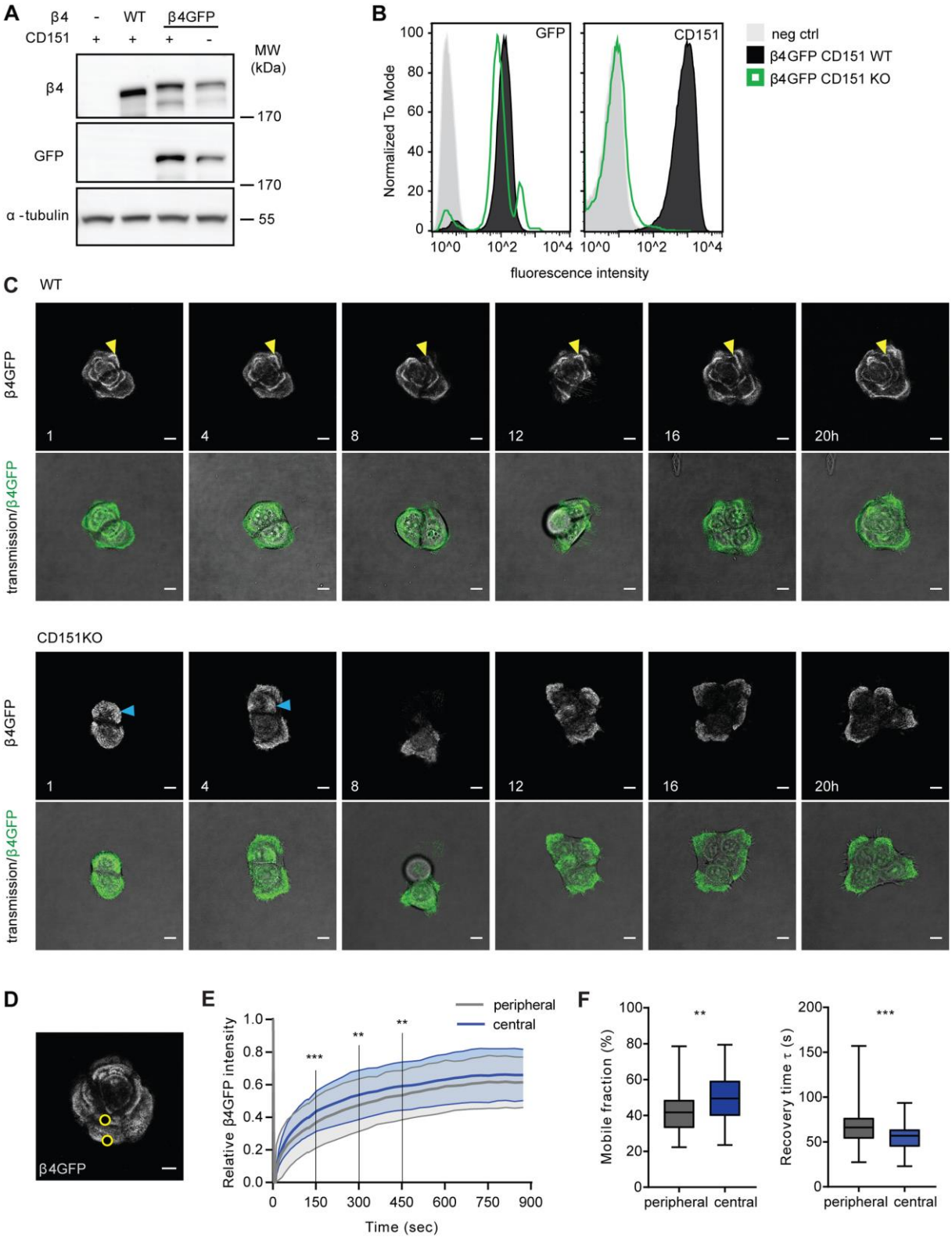

Fig. 3. CD151 is essential for maintenance of early α6β4-containing adhesions

(A) WB analyses of WT or CD151-KO PA-JEB keratinocytes, reconstituted with WT-β4 or β4-GFP. Whole cell lysates were tested for β4, GFP and α-tubulin protein levels. (B) FACS analyses of CD151 and β4-GFP surface expression on CD151-KO and WT PA-JEB/β4-GFP cells. (C) Stills from a time-lapse

experiment using WT and CD151-KO PA-JEB/β4-GFP cells. Top panels show the β4-GFP signal and bottom panels the overlay of the β4-GFP and DIC signal. Stills show images taken at 1, 4, 8, 12, 16 and 20 hours after addition of DMEM+FCS (0h time point, 20h after seeding). The yellow arrowheads indicate a peripheral adhesion becoming a central adhesion over time in WT cells and the blue arrowheads indicate a peripheral adhesion disappearing over time in KO cells. Scale bars are 10 µm. (D) Example image of PA-JEB/β4-GFP after the bleach step of a FRAP experiment; FRAP regions indicated in peripheral and central adhesions with yellow circles. Scale bar is 10 µm. (E) The relative β4-GFP intensity over time (in seconds) during FRAP experiments in both central (blue) and peripheral (grey) α6β4-containing adhesions. Data was collected from 38 islands in 3 experiments., lineplot shows the mean+s.d and P values are **< 0.01, ***< 0.001 (Wilcoxon matched-pairs signed rank test). (F) Mobile fraction and recovery time of β4-GFP in central and peripheral adhesions during the first 230 seconds of the same dataset used for E. Graph: boxplots dividing the data in quartiles and significance was calculated the same as for E.

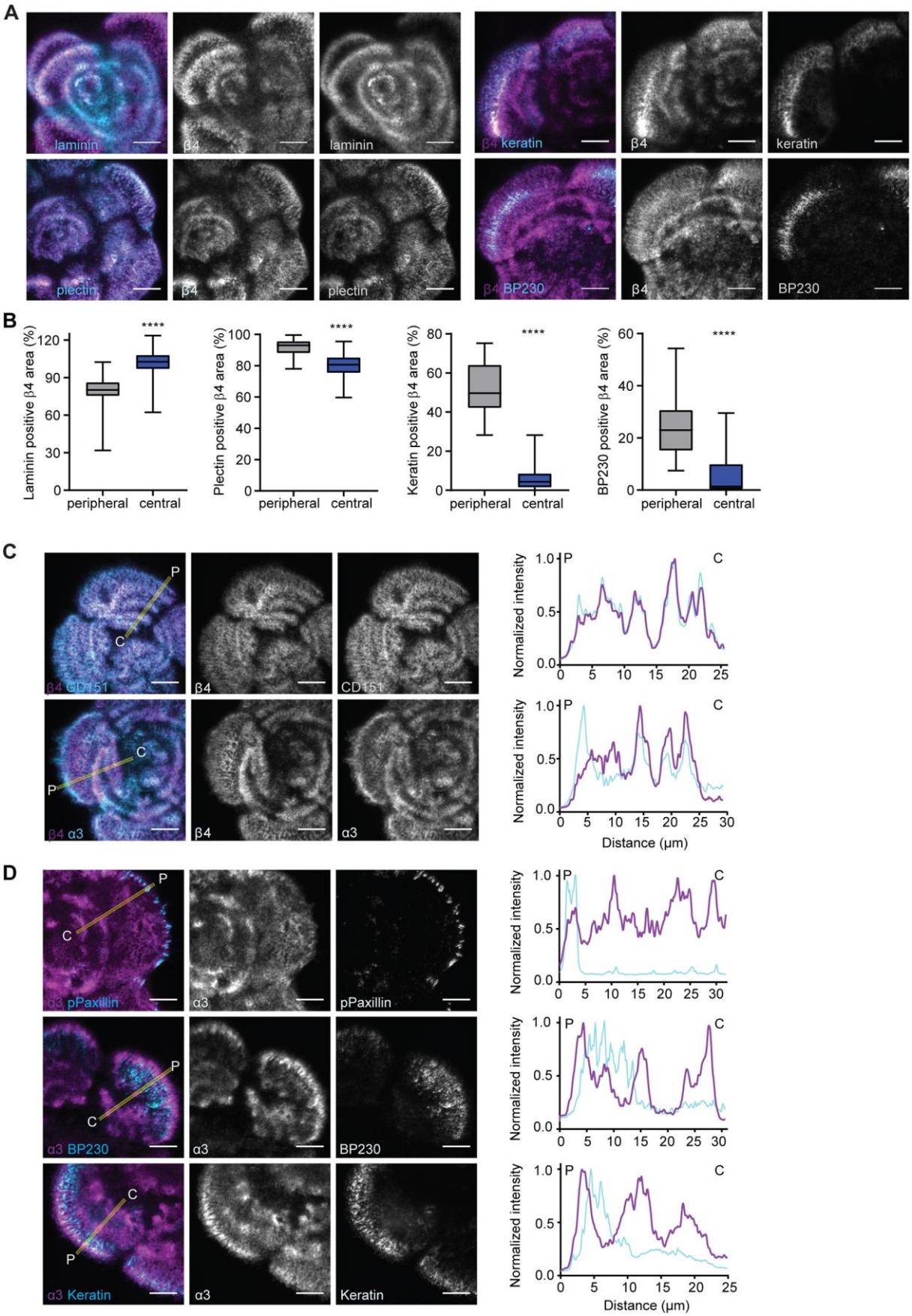

Fig. 4. Central and peripheral adhesions differ in protein composition

(A) TIRF images of PA-JEB/β4 keratinocytes stained for β4 (magenta) and laminin-332, plectin, keratin-14 or BP230 (cyan). Scale bars are 10 µm. (B) Quantification of the β4 area which is positive for laminin-332 (57 images; 2 exp.), plectin (60 images; 2 exp.), keratin-14 (59 images; 2 exp.) or BP230 (61 images; 2 exp.) in peripheral and central α6β4-containing adhesions. Graph: boxplots dividing the data in quartiles; P value: ****< 0.0001 (Mann-Whitney U test). (C) TIRF images of PA-JEB/β4 cells stained for β4 (magenta) and CD151 or α3 (cyan). Scale bars are 10 µm. (C+D) Line plot shows the normalized intensities of the different proteins along the line (thickness: 10 pixels) indicated in the overlay image. The line starts in the periphery and is drawn towards the center of the island. (D) TIRF images of PA-JEB/β4 cells stained for α3 (magenta) and phosphorylated paxillin, BP230 or keratin (cyan). Scale bars are 10 µm.

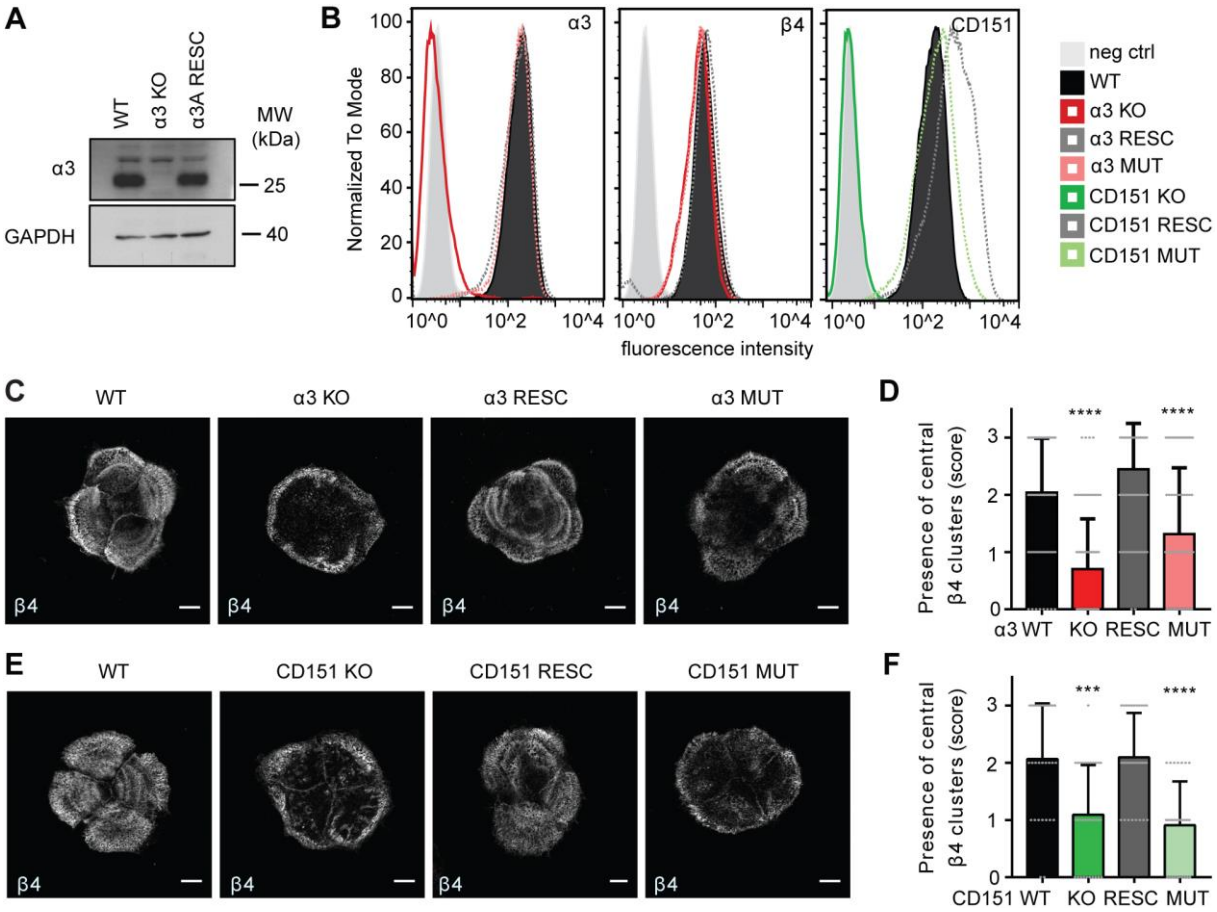

Fig. 5. α3β1 and CD151-self association contribute to stabilization of central HD-like adhesions.

(A) Whole cell lysate of WT, α3-KO and α3-RESC HaCaT keratinocytes analyzed for protein levels of α3 and GAPDH (loading control) by WB. (B) FACS analyses of α3, β4 or CD151 surface expression on WT, α3-KO/-RESC/-MUT and CD151-KO/-RESC/-MUT HaCaT keratinocytes. (C) Confocal images of β4 in WT and α3-KO/-RESC/-MUT HaCaT keratinocytes. Scale bars are 10 µm. (D) Quantification of the presence of central β4 clusters (score 0-3) in WT (101 islands; 4 exp.) and α3-KO (98 islands; 4 exp.) /-RESC (103 islands; 4 exp.) /-MUT (102 islands; 4 exp.) HaCaT keratinocytes. Graph: Mean+s.d.; P value: ****< 0.0001 (Mann-Whitney U test) (E) Confocal images of β4 in WT and CD151-KO/-RESC/-MUT HaCaT cells. Scale bars are 10 µm. (F) Quantification of the presence of central β4 clusters (score 0-3) in WT (31 islands; 2 exp.) and CD151-KO (33 islands; 2 exp.)/-RESC (32 islands; 2 exp.)/-MUT (33 islands; 2 exp.) cells. Graph: Mean+s.d.; P values: ***< 0.001, ****< 0.0001 (Mann-Whitney U test).

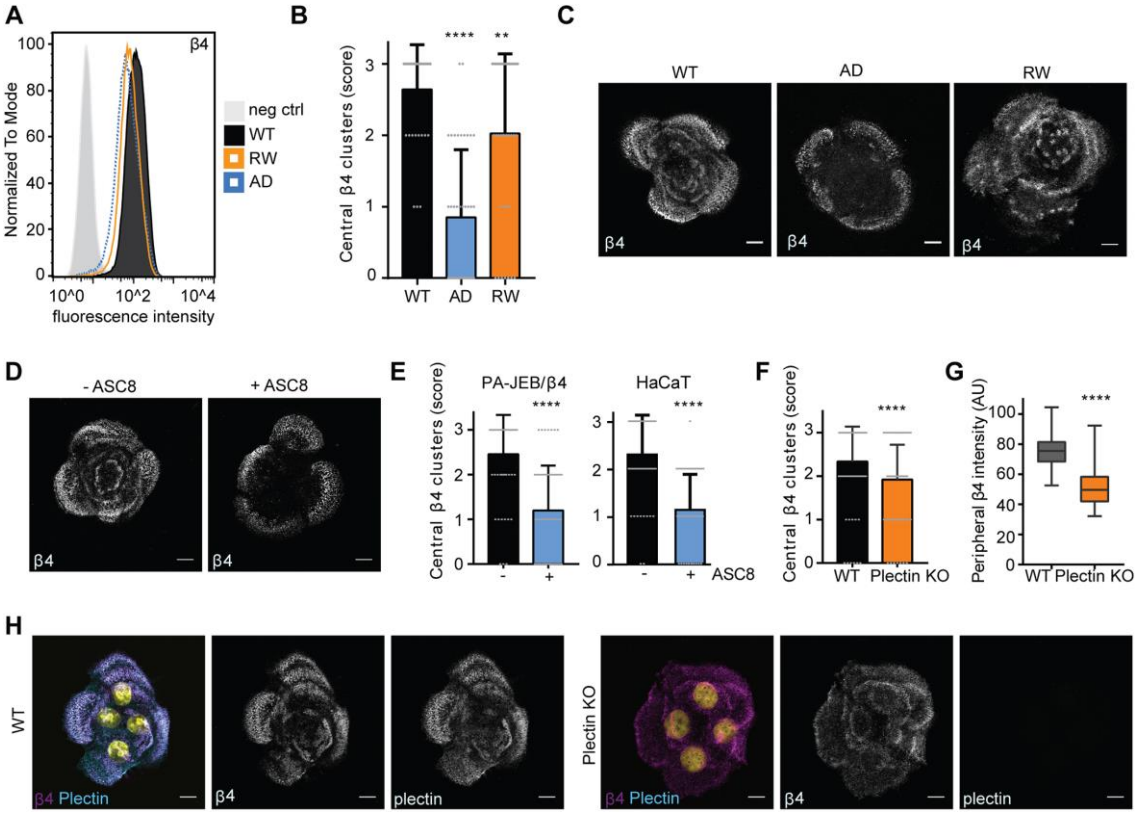

Fig. 6. Laminin- but not plectin binding to α6β4 contributes to stabilization of central HD-like adhesions

(A) FACS analyses of β4 surface expression on WT/β4-AD/β4-RW expressing PA-JEB keratinocytes. (B) Quantification of the central β4 clusters (score 0-3) in WT (39 images; 3 exp.), β4-AD (40 images; 3 exp.) and β4-RW (42 images; 3 exp.). Graph: Mean+s.d.; P values: **< 0.01, ****< 0.0001 (Mann-Whitney U test). (C) Confocal images of β4 in WT and β4-AD/β4-RW PA-JEB/β4 keratinocytes. Scale bars are 10 µm. (D) Confocal images of β4 in WT PA-JEB/β4 keratinocytes grown on coverslips for two days in the absence (-) or presence (+) of β4 blocking antibody ASC8. Scale bars are 10 µm. (E) Quantification of the presence of central β4 clusters (score 0-3) in WT PA-JEB/β4 treated without (59 images; 3 exp.) or with (60 images; 3 exp.) ASC8 and HaCaT keratinocytes treated without (60 images; 3 exp.) or with (60 images; 3 exp.) ASC8. Graph: Mean+s.d.; P value: ****< 0.0001 (Mann-Whitney U test). (F) Quantification of the presence of central β4 clusters (score 0-3) in WT (110 images; 6 exp.) and plectin-KO (102 images; 6 exp.) PA-JEB/β4 keratinocytes. Graph: Mean+s.d.; P value: ****< 0.0001 (Mann-Whitney U test). (G) Quantification of the mean intensity of β4 clustered in the peripheral adhesions in WT (73 images: 4 exp.) and plectin-KO (71 images; 4 exp.) PA-JEB/β4 cells. Graph: boxplots dividing the data in quartiles; P value: ****< 0.0001 (Mann-Whitney U test). (H) Confocal images of β4 (magenta) and plectin (cyan) in WT and plectin-KO PA-JEB/β4 keratinocytes. Scale bars are 10 µm.

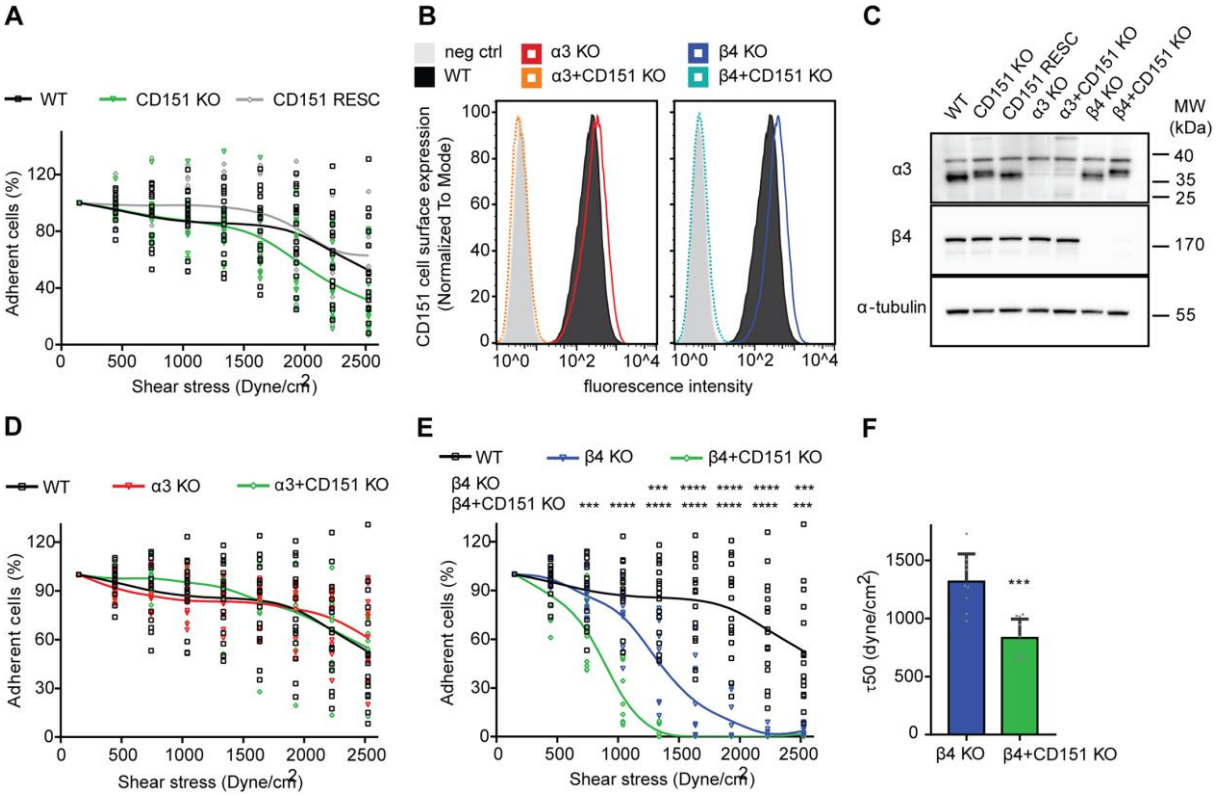

Fig. 7. CD151 contributes to α3β1-mediated adhesion strengthening.

(A) Percentage of WT (squares; n=16), CD151-KO (triangles; n=13) and CD151-RESC (diamonds; n=14) HaCaT keratinocytes that remained adherent under conditions of increasing shear stresses (shown in dynes/cm^2). Graph: The line depicts the mean; no significant differences (unpaired T-tests corrected for multiple comparisons). (B) CD151 surface expression of WT, α3-KO, β4-KO and double α3+CD151 and β4+CD151 KO HaCaT keratinocytes analyzed by FACS. (C) Expression of α3, β4 and α-tubulin (loading control) in whole cell lysates from WT, CD151-KO and CD151-RESC, α3-KO, β4-KO and double α3+CD151 and β4+CD151 KO HaCaT keratinocytes analyzed by WB. (D,E) Percentage of WT (squares; n=16), α3-KO (triangles; n=11) and double α3+CD151 KO (diamonds; n=11) HaCaT keratinocytes (D) and of WT (squares; n=16), β4-KO (triangles; n=9) and double β4+CD151 KO (diamonds; n=10) HaCaT keratinocytes (E) that remained adherent after being submitted to increasing conditions of shear stresses (in dynes/cm^2). Graph: The line depicts the mean; P values: ***<0.001, ****< 0.0001 (unpaired T-tests corrected for multiple comparisons). (F) τ50 calculated for β4-KO and double β4+CD151 KO HaCaT cells from the same dataset shown in (E). Graph: Mean+s.d.; P value: ***< 0.001 (Mann-Whitney U test).

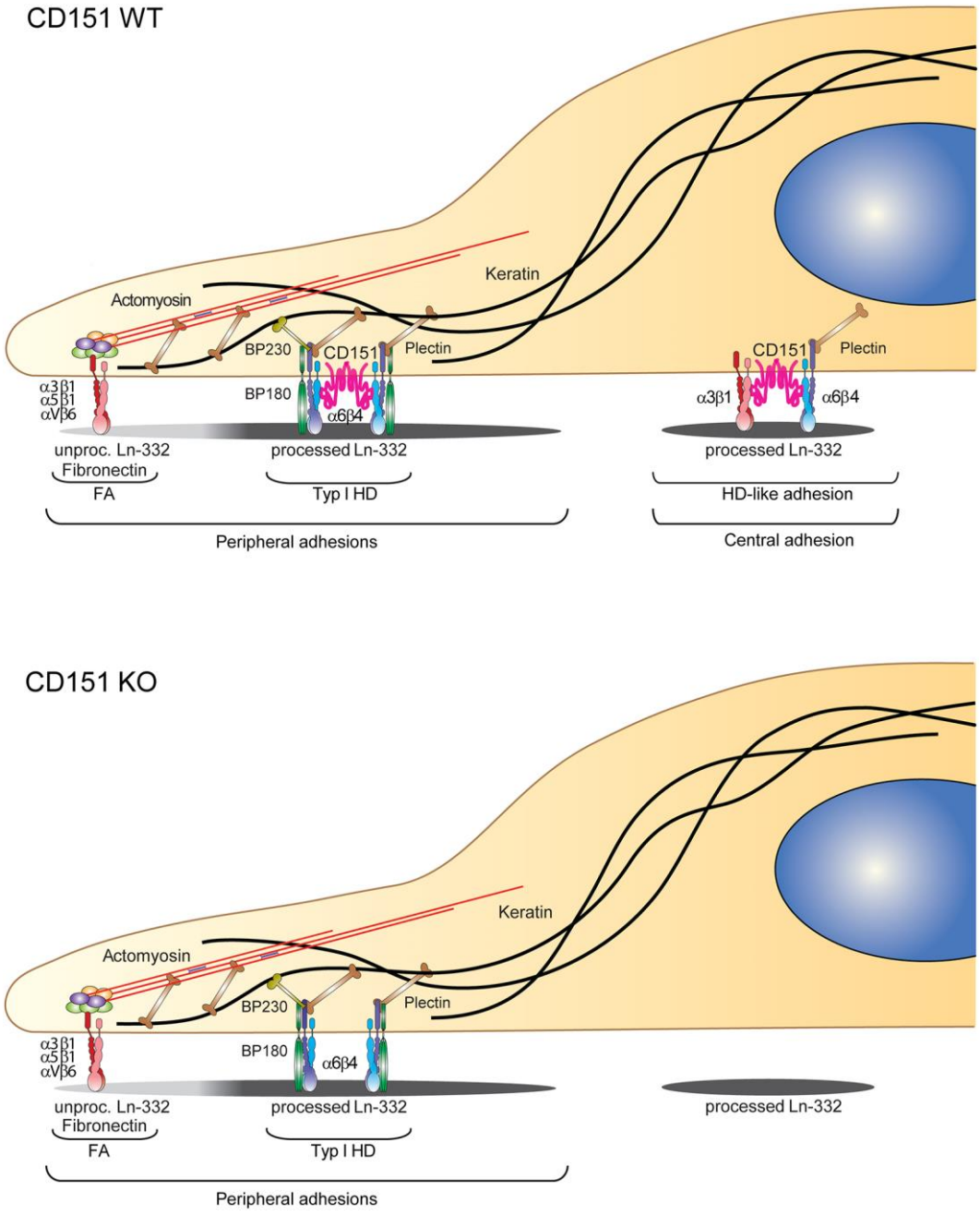

Fig. 8. CD151 is essential for the maintenance of central HD-like adhesions but not the formation of peripheral FAs and type I HDs.

In the presence of CD151 (top panel), α3β1 and α6β4 are present together with CD151 in central HD-like adhesions. Additionally, α3β1 is present in FAs in the periphery of the cell island preceding the type I HDs in which α6β4 is present also together with CD151. In the absence of CD151 (bottom panel), the peripheral adhesions are still formed but lack CD151, while the central HD-like adhesions are lost.

Target	Antibody	Application	Source/kind gift from
α-tubulin	Mouse mAb	WB (1:10000)	Sigma #t5168
BP230	5E, human mAb	IF (1:400)	Takashi Hashimoto
CD151	5C11, mouse mAb	IF (1:1), IP (1:5), WB (1:50)	Fedor Berditchevski
Coll. XVII	VK14, mouse mAb	IF (1:5)	Hendri Pas
CD151	11G5 (IgG1), mouse mAb	IP (1 µg ml^{-1}), FACS (1:400), WB (1:2000)	Jonathan Humphries
CD151	11B1.G4 (p48), mouse mAb	WB (1:2500)	Leonie Ashman
GAPDH	Rabbit pAb	WB (1:2000)	Cell Signaling #5174
GFP	Mouse mAb	WB (1:5000)	Covance
Itg. α3	J143, mouse mAb	IF (1:250), IP (1 µg ml^{-1}), FACS (1:400), blocking (30 µg ml^{-1})	American Type Culture Collection
Itg. α3	A-3, mouse (IgG2a) mAb	IF (1:100)	Santa Cruz #sc-374242
Itg. α3A	Rabbit pAb	WB (1:1000)	Homemade
Itg. α6	AA6NT, rabbit pAb	WB (1:500)	Anne Cress
Itg. α6	GoH3, rat mAb	IP (1 µg ml^{-1})	Homemade
Itg. β1	Rabbit pAb	WB (1:2000)	Reinhard Fässler
Itg. β4	439-9B, rat mAb	IF (1:200)	BD Bioscience #555719
Itg. β4	PE-Rat anti-human-CD104	FACS (1:400)	BD Pharmingen #555720
Itg. β4	ASC8, mouse, mAb	Blocking (1:5)	Amy Skubitz
Itg. β4	Rabbit pAb	WB (1:2000)	Homemade
Keratin 14	Rabbit pAb	IF (1:1000)	Covance #PRB-155P
Laminin-332	R14, rabbit pAb	IF (1:500)	Monique Aumailley
pPaxillin Y31	Rabbit pAb	IF (1:200)	Biosource #44-720G
Plectin	P2, guinea pig pAb	IF (1:400)	Harald Herrmann

Table S1. Primary antibodies used in various techniques
Abbreviations used: Immune fluorescence (IF), Immune precipitation (IP), fluorescence-activated cell sorting (FACS) and Western blot (WB).

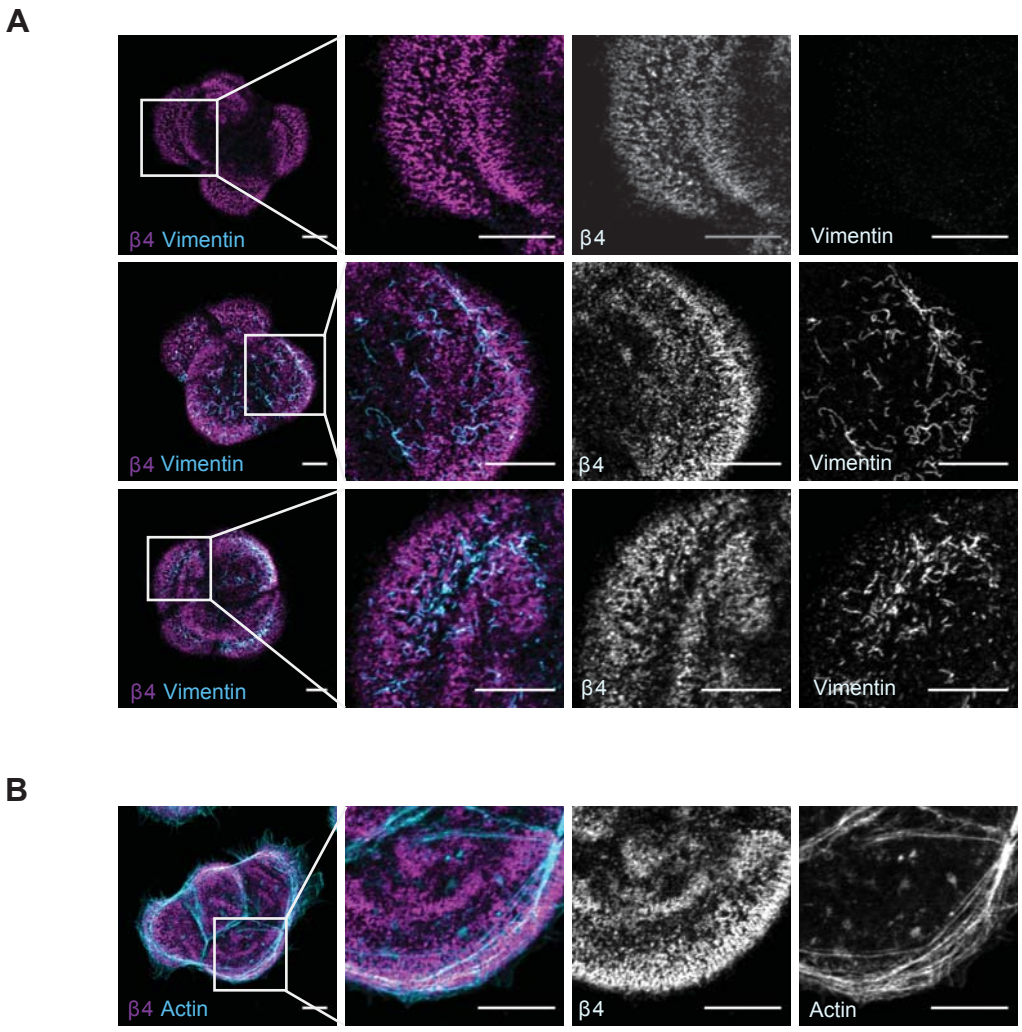

Fig. S1 α6β4 in central HD-like adhesions is not associated with actin or vimentin.
Example overview and zoom-in confocal images of PA-JEB/β4 keratinocytes stained for β4 (magenta) and vimentin (A) or actin (B) (cyan). Top panel of A represents the ~ 50% of PA-JEB/β4 keratinocyt cell islands in which vimentin is absent. Scale bars are 10 µm.

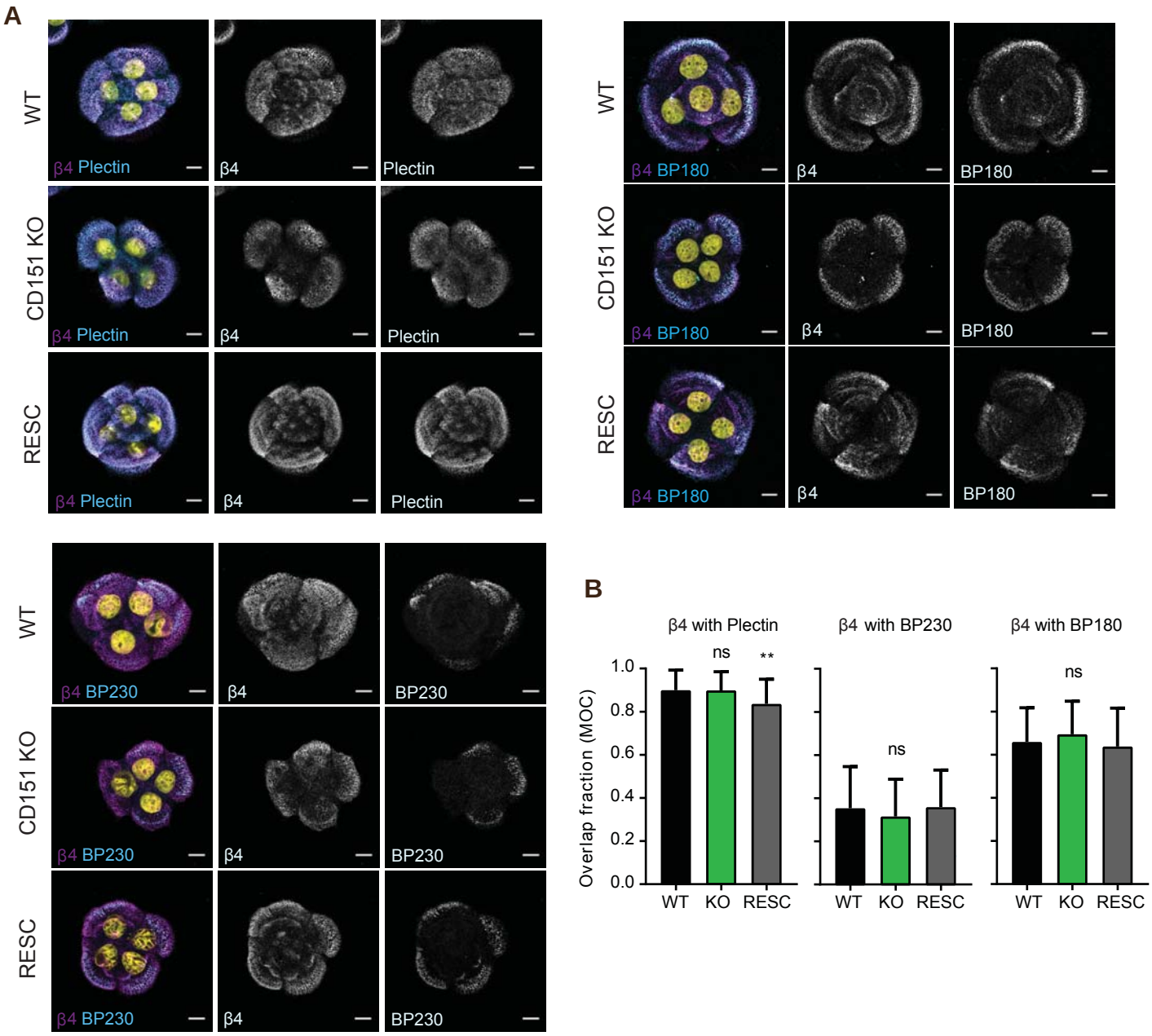

Fig. S2 Type I HDs are formed in the absence of CD151.
(A) Confocal images of WT, CD151-KO and CD151-RESC PA-JEB/β4 keratinocytes stained for plectin, BP180 or BP230 (cyan), β4 (magenta) and DAPI (yellow). Scale bars are 10 µm. B. Quantification of the colocalization (MOC) of β4 with BP180 (WT: 52 images, KO: 47 images, RESC: 48 images; 2 exp. each), BP230 (WT: 97 images, KO: 90 images, RESC: 89 images; 5 exp. each) and plectin (WT: 46 images, KO: 42 images, RESC: 41 images; 3 exp. each) in WT, CD151-KO and CD151-RESC PA-JEB/β4 keratinocytes. Graphs show the mean+s.d.; P value: **< 0.01 (Mann-Whitney U test), ns>0.05.

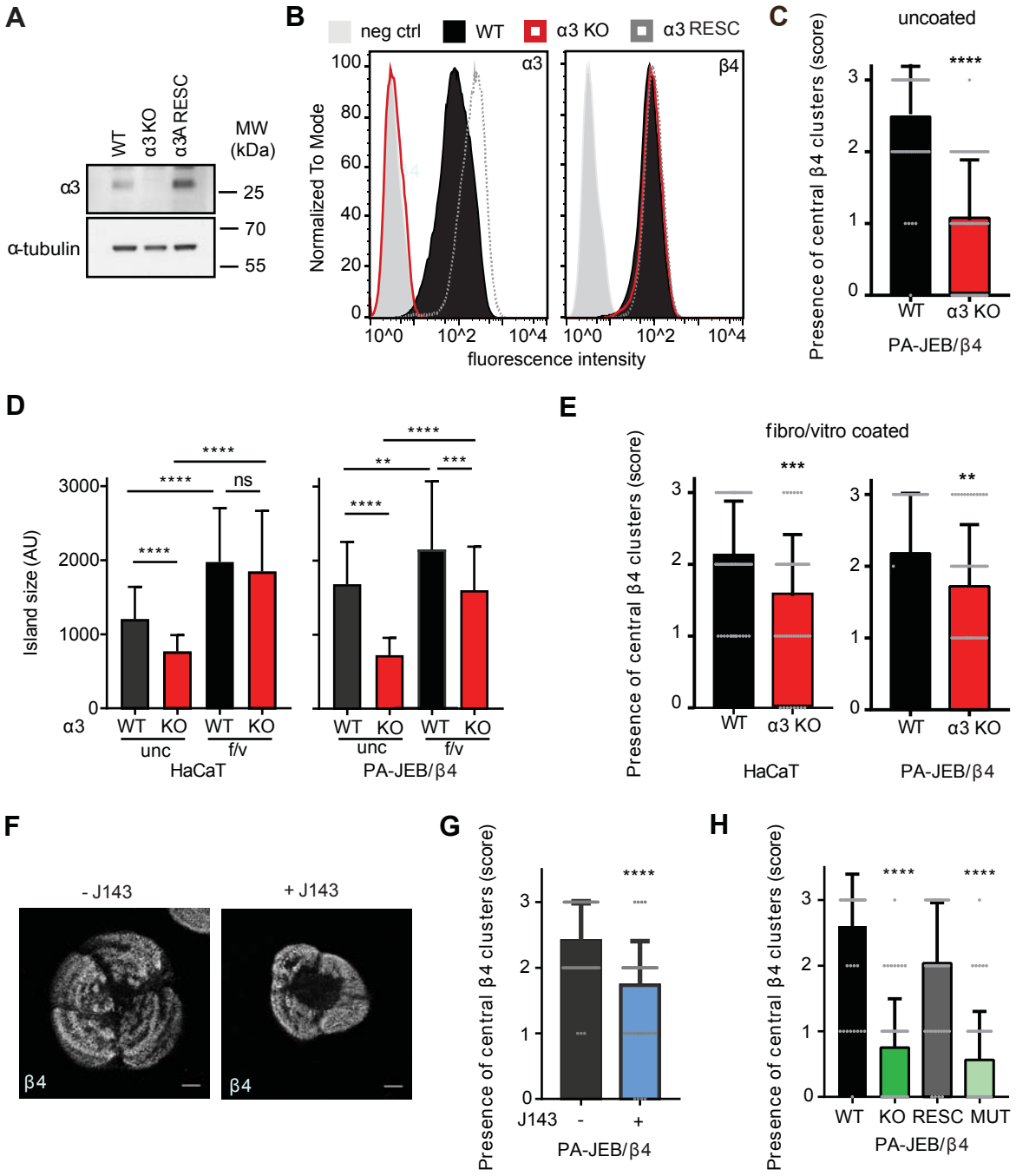

Fig. S3 Confirmation of α3β1 involvement in the maintenance of central HD-like adhesions.
(A) Whole cell lysate of WT, α3-KO and α3-RESC PA-JEB/β4 keratinocytes analyzed by WB for protein levels of α3 and GAPDH (loading control). (B) FACS analyses of α3 and β4 surface expression on WT, α3-KO and α3-RESC PA-JEB/β4 keratinocytes. (C) Quantification of the presence of central β4 clusters (score 0-3) in WT (61 images; 3 exp.) and α3-KO (62 images; 3 exp.) PA-JEB/β4 keratinocytes. (D) Island size of WT and α3-KO HaCaT and PA-JEB/β4 keratinocytes seeded on uncoated (unc) or fibronectin and vitronectin (f/v) coated coverslips (~60 images each; 3 exp.). (E) Quantification of the presence of central β4 clusters (score 0-3) in WT (60 images; 3 exp.) and α3-KO (59 images; 3 exp.) HaCaT keratinocytes, and WT (60 images; 3 exp.) and α3-KO (61 images; 3 exp.) PA-JEB/β4 keratinocytes seeded on fibronectin and vitronectin coated coverslips. (F) Confocal images of β4 in PA-JEB/β4 cells grown on coverslips for two days in the absence (-) or presence (+) of α3 blocking antibody J143. Scale bars are 10 µm. (G) Quantification of the presence of central β4 clusters (score 0-3) in WT PA-JEB/β4 cells grown in the absence (65 images; 3 exp.) or presence (66 images; 3 exp.) of J143. (H) Quantification of the presence of central β4 clusters (score 0-3) in WT (57 images; 4 exp), CD151-KO (56 images; 4 exp.), RESC (55 images; 4 exp.) and MUT (55 images; 4 exp.) PA-JEB/β4 keratinocytes. WT, KO and RESC data is identical to the data depicted in Fig. 2G. Graphs in C, D, E, G and H show the mean+s.d.; P values: **<0.01, ***< 0.001, ****< 0.0001 (Mann-Whitney U test).

Movie 1
Movies of a time-lapse experiment using WT (movie S1) and CD151-KO (movie S2) PA-JEB/β4-GFP keratinocytes. Images were taken every hour for 20h, starting from the addition of DMEM+FCS (0h timepoint, 20h after seeding).

Movie 2
Movies of a time-lapse experiment using WT (movie S1) and CD151-KO (movie S2) PA-JEB/β4-GFP keratinocytes. Images were taken every hour for 20h, starting from the addition of DMEM+FCS (0h timepoint, 20h after seeding).

Journal of Cell Science • Supplementary information

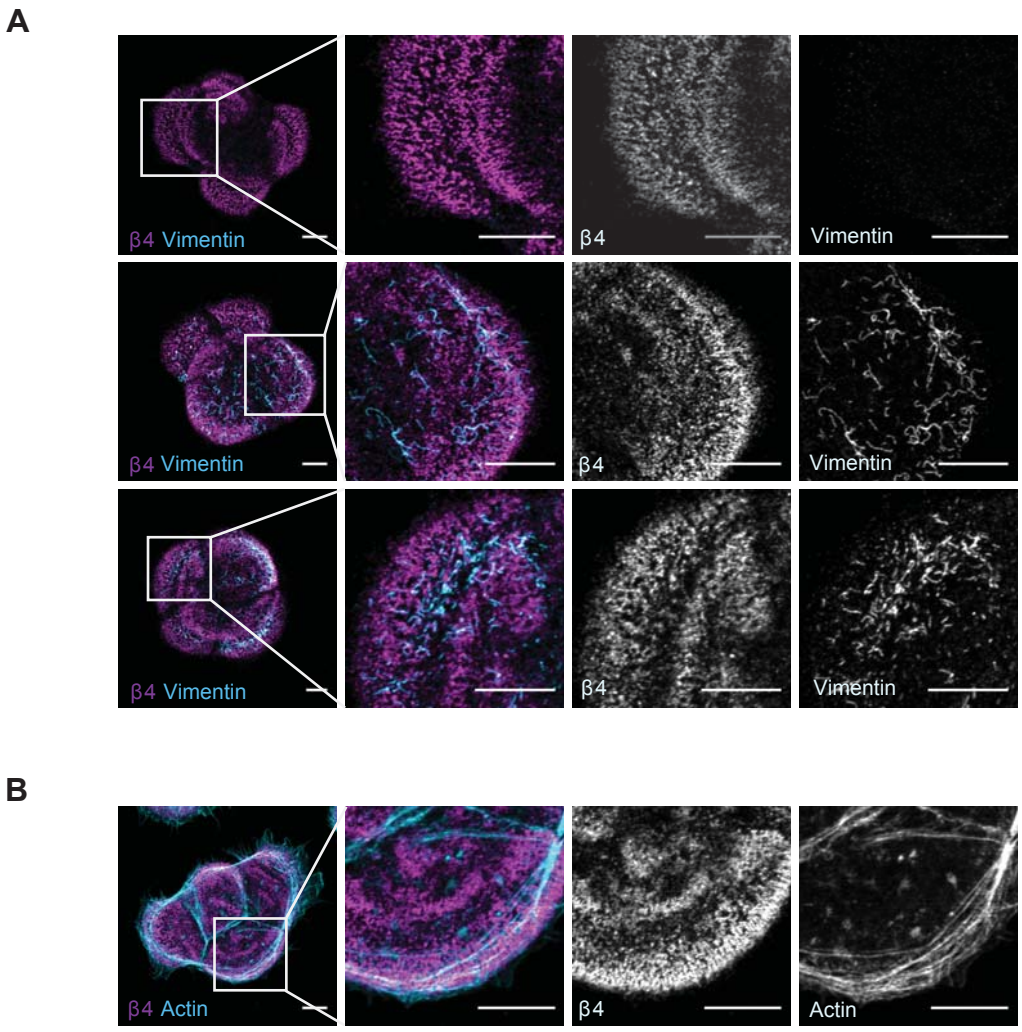

Fig. S1 α6β4 in central HD-like adhesions is not associated with actin or vimentin.
Example overview and zoom-in confocal images of PA-JEB/β4 keratinocytes stained for β4 (magenta) and vimentin (A) or actin (B) (cyan). Top panel of A represents the ~ 50% of PA-JEB/β4 keratinocyt cell islands in which vimentin is absent. Scale bars are 10 µm.

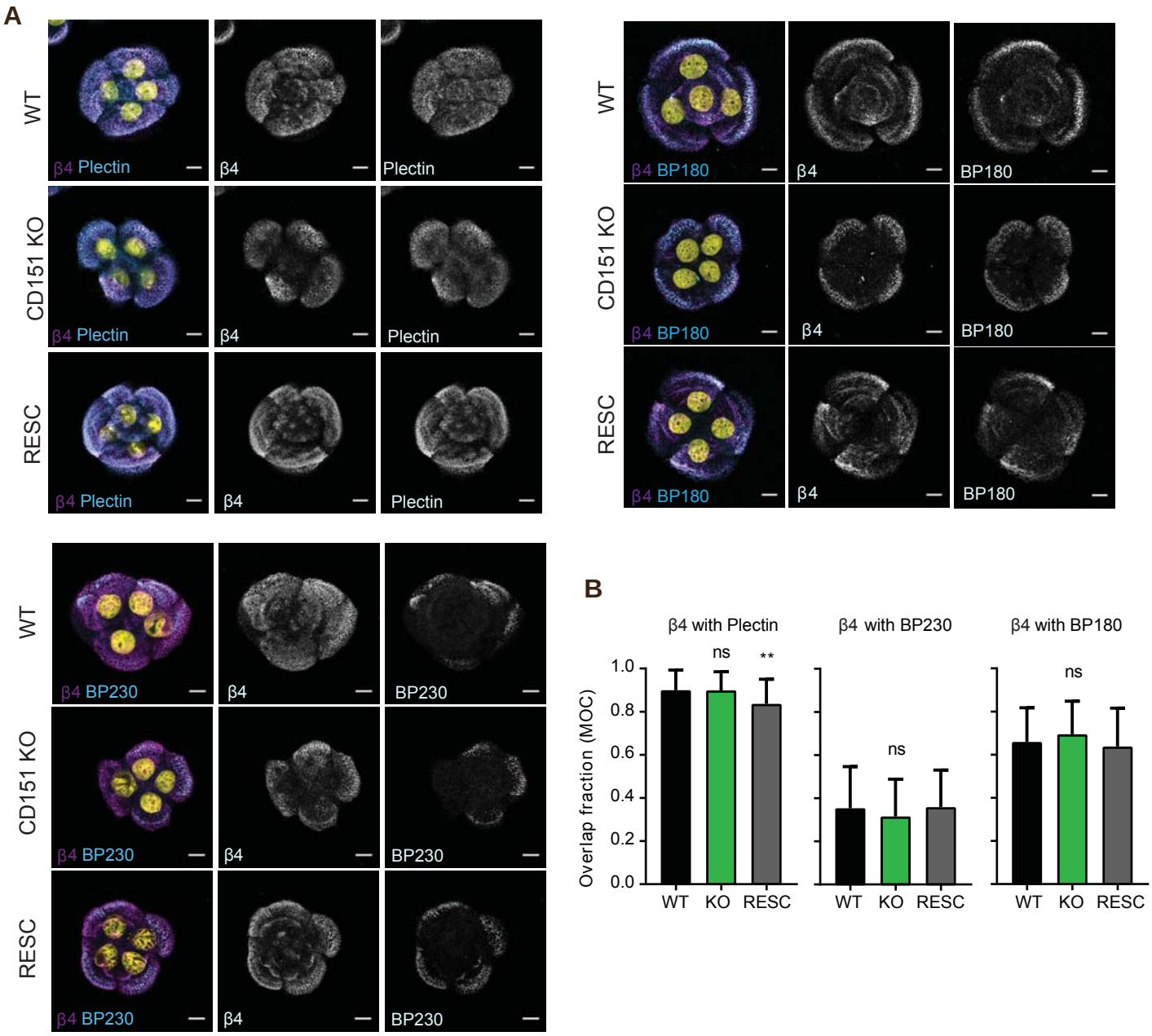

Fig. S2 Type I HDs are formed in the absence of CD151.
(A) Confocal images of WT, CD151-KO and CD151-RESC PA-JEB/β4 keratinocytes stained for plectin, BP180 or BP230 (cyan), β4 (magenta) and DAPI (yellow). Scale bars are 10 µm. B. Quantification of the colocalization (MOC) of β4 with BP180 (WT: 52 images, KO: 47 images, RESC: 48 images; 2 exp. each), BP230 (WT: 97 images, KO: 90 images, RESC: 89 images; 5 exp. each) and plectin (WT: 46 images, KO: 42 images, RESC: 41 images; 3 exp. each) in WT, CD151-KO and CD151-RESC PA-JEB/β4 keratinocytes. Graphs show the mean+s.d.; P value: **< 0.01 (Mann-Whitney U test), ns>0.05.

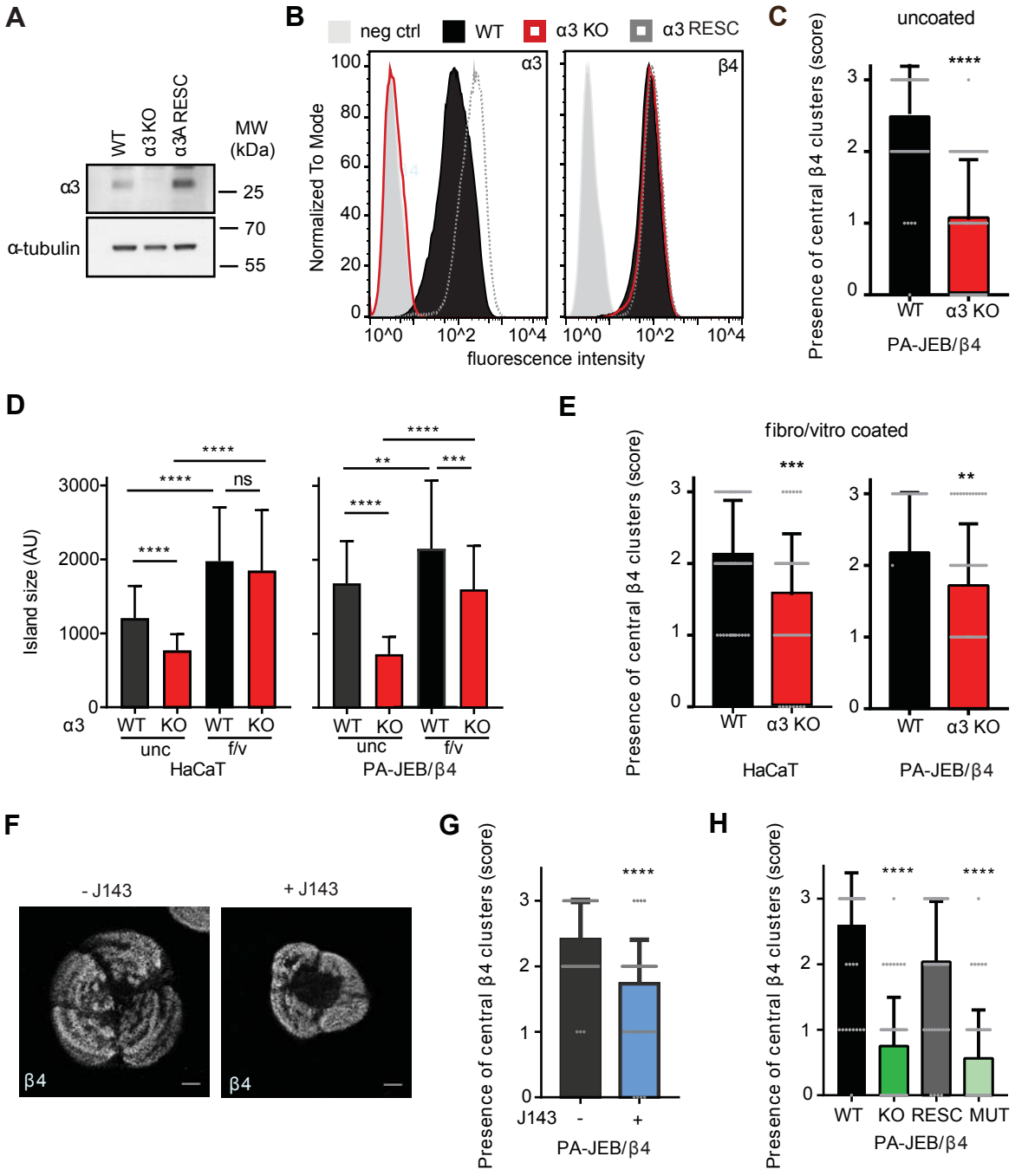

Fig. S3 Confirmation of α3β1 involvement in the maintenance of central HD-like adhesions.
(A) Whole cell lysate of WT, α3-KO and α3-RESC PA-JEB/β4 keratinocytes analyzed by WB for protein levels of α3 and GAPDH (loading control). (B) FACS analyses of α3 and β4 surface expression on WT, α3-KO and α3-RESC PA-JEB/β4 keratinocytes. (C) Quantification of the presence of central β4 clusters (score 0-3) in WT (61 images; 3 exp.) and α3-KO (62 images; 3 exp.) PA-JEB/β4 keratinocytes. (D) Island size of WT and α3-KO HaCaT and PA-JEB/β4 keratinocytes seeded on uncoated (unc) or fibronectin and vitronectin (f/v) coated coverslips (~60 images each; 3 exp.). (E) Quantification of the presence of central β4 clusters (score 0-3) in WT (60 images; 3 exp.) and α3-KO (59 images; 3 exp.) HaCaT keratinocytes, and WT (60 images; 3 exp.) and α3-KO (61 images; 3 exp.) PA-JEB/β4 keratinocytes seeded on fibronectin and vitronectin coated coverslips. (F) Confocal images of β4 in PA-JEB/β4 cells grown on coverslips for two days in the absence (-) or presence (+) of α3 blocking antibody J143. Scale bars are 10 µm. (G) Quantification of the presence of central β4 clusters (score 0-3) in WT PA-JEB/β4 cells grown in the absence (65 images; 3 exp.) or presence (66 images; 3 exp.) of J143. (H) Quantification of the presence of central β4 clusters (score 0-3) in WT (57 images; 4 exp), CD151-KO (56 images; 4 exp.), RESC (55 images; 4 exp.) and MUT (55 images; 4 exp.) PA-JEB/β4 keratinocytes. WT, KO and RESC data is identical to the data depicted in Fig. 2G. Graphs in C, D, E, G and H show the mean+s.d.; P values: **<0.01, ***< 0.001, ****< 0.0001 (Mann-Whitney U test).

Target	Antibody	Application	Source/kind gift from
α-tubulin	Mouse mAb	WB (1:10000)	Sigma-Aldrich #t5168
BP230	5E, human mAb	IF (1:400)	Takashi Hashimoto, Keio University School of Medicine, Shinjuku, Tokyo, Japan
Coll. XVII	VK14, mouse mAb	IF (1:5)	Hendri Pas University Medical Center Groningen, Groningen, The Netherlands
CD151	5C11, mouse mAb	IF (1:1), IP (1:5), WB (1:50)	Fedor Berditchevski University of Birmingham, Birmingham, United Kingdom
CD151	11G5 (IgG1), mouse mAb	IP (1 µg ml^{-1}), FACS (1:400), WB (1:2000)	Jonathan Humphries University of Manchester, Manchester, United Kingdom
CD151	11B1.G4 (p48), mouse mAb	WB (1:2500)	Leonie Ashman University of Newcastle, Newcastle, NSW, Australia.
GAPDH	Rabbit pAb	WB (1:2000)	Cell Signaling #5174
GFP	B34, mouse mAb	WB (1:5000)	Covance
Itg. α3	J143, mouse mAb	IF (1:250), IP (1 µg ml^{-1}), FACS (1:400), blocking (30 µg ml^{-1})	American Type Culture Collection
Itg. α3	A-3, mouse (IgG2a) mAb	IF (1:100)	Santa Cruz #sc-374242
Itg. α3A	Rabbit pAb	WB (1:1000)	In-house
Itg. α6	AA6NT, rabbit pAb	WB (1:500)	Anne Cress University of Arizona, Tucson, Arizona, USA
Itg. α6	GoH3, rat mAb	IP (1 µg ml^{-1})	In-house
Itg. β1	Rabbit pAb	WB (1:2000)	Reinhard Fässler Max Planck Institute of Biochemistry, Martinsried, Germany
Itg. β4	439-9B, rat mAb	IF (1:200)	BD Bioscience #555719
Itg. β4	PE-rat anti-human-CD104	FACS (1:400)	BD Pharmingen #555720
Itg. β4	ASC8, mouse, mAb	Blocking (1:5)	Amy Skubitz University of Minnesota, Minneapolis, MN, USA
Itg. β4	Rabbit pAb	WB (1:2000)	In-house
Keratin 14	Rabbit pAb	IF (1:1000)	Covance #PRB-155P
Laminin-332	R14, rabbit pAb	IF (1:500)	Monique Aumailley University of Cologne, Cologne, Germany
pPaxillin Y31	Rabbit pAb	IF (1:200)	Biosource #44-720G
Plectin	P2, guinea pig pAb	IF (1:400)	Harald Herrmann German Cancer Research Center, Heidelberg, Germany

Table S1. Primary antibodies used in various techniques
Abbreviations used: Immune fluorescence (IF), Immune precipitation (IP), fluorescence-activated cell sorting (FACS) and Western blot (WB).

Movie 1
Movies of a time-lapse experiment using WT (movie S1) and CD151-KO (movie S2) PA-JEB/β4-GFP keratinocytes. Images were taken every hour for 20h, starting from the addition of DMEM+FCS (0h timepoint, 20h after seeding).

Movie 2
Movies of a time-lapse experiment using WT (movie S1) and CD151-KO (movie S2) PA-JEB/β4-GFP keratinocytes. Images were taken every hour for 20h, starting from the addition of DMEM+FCS (0h timepoint, 20h after seeding).

Journal of Cell Science • Supplementary information